STIC-ILL

pg 1 of 0 7/23

From: Gambel, Phillip
Sent: Tuesday, July 23, 2002 4:00 PM
To: STIC-ILL
Subject: refernces of recrod in ussn 09 / 010377 rubin encephalitis

405028

stic

please provide the following references to

phillip gambel
art unit 1644
308-3997

1644 mailbox 9E12

---

1) sanders et al. archives of neurology 53 : 125- 133 (1996)

2) editorial archives of neurology 53 : 123- 124 (1996)

3) soilo-hanninen et al. scand. j. immunol. 43 : 727 - ? (1996)

4) soilo-hanninen et al. j. neuroimmunol. 72 : 95 - 105 (1997)

5) planz et al. j. virol. 69 : 896 - 903 (1995)

thanx

ADONIS NOS

~~QR180.533~~

(4)

•364 A&L
7-25=R.C

Immunology

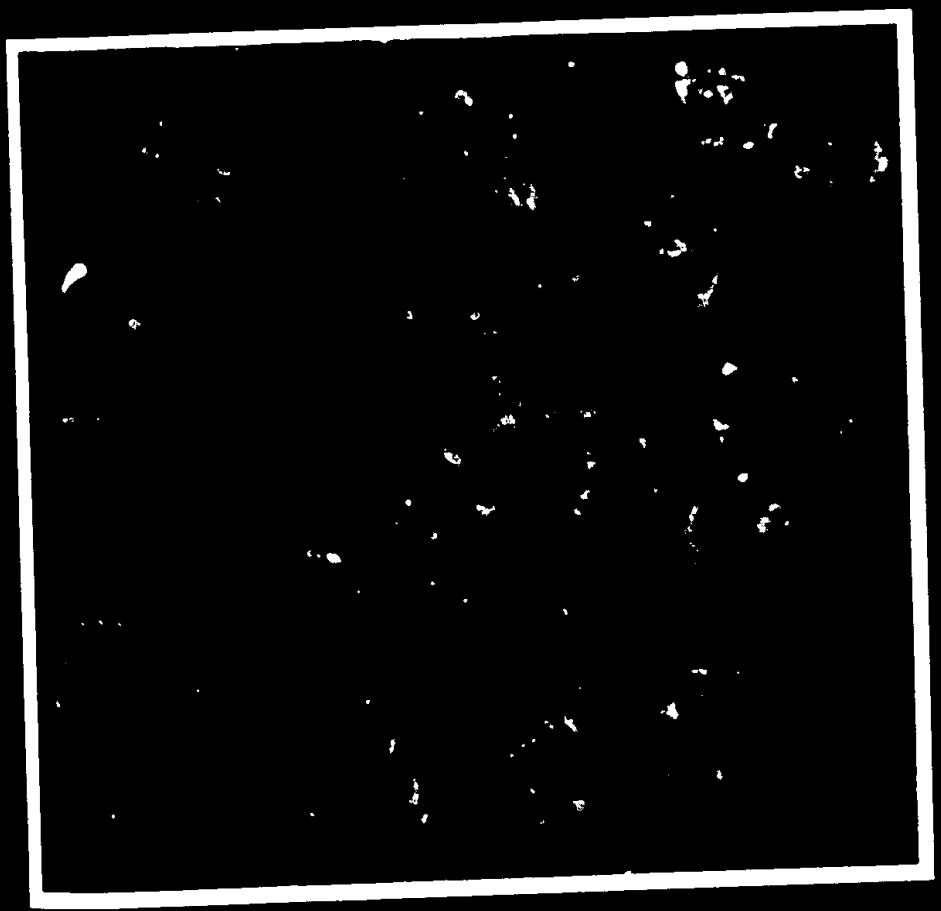

Blackwell Science

136 THERAPY WITH ANTIBODY AGAINST LEUKOCYTE INTEGRIN VLA-4 IS EFFECTIVE AND SAFE IN VIRUS FACILITATED EAE

Merja Soilu-Hänninen, Matias Röyttä, Aimo Salmi and Reijo Salonen. Departments of Virology and Pathology, University of Turku, Kiinamyllynkatu 13, 20520 Turku, Finland.
Fax +358-21-2513303

Experimental allergic encephalomyelitis (EAE) is facilitated in resistant BALB/c mice by intraperitoneal infection with an avirulent Semliki Forest virus (SFV-A7). Virus infection increases incidence of EAE from 15-30% to 60-90% and speeds up appearance of paralysis from 24 to 14 days. In this paper, we describe treatment of virus facilitated EAE with monoclonal antibodies (mAbs) against leukocyte and/or endothelial cell adhesion molecules. Therapy with mAb against ICAM-1 (intercellular adhesion molecule-1) had a modest effect, but caused hemorrhagic brain and spinal cord lesions. Therapy with mAb against Mac-1 (macrophage adhesion promoting receptor) was well tolerated but ineffective. Therapy with mAb against VLA-4 (very late antigen-4) was safe, dimished both clinical and histopathological signs of EAE, decreased induction of VCAM-1 (vascular cell adhesion molecule-1) on brain vessels and dimished infiltration of VLA-4$^+$ leukocytes into the brain. The amount of viral antigen was not altered. We conclude that facilitation of leukocyte entry into the brain is a major mechanism for viral facilitation of EAE in the BALB/c mouse, and that facilitation can inhibited by anti-adhesion therapy. This may have implications for treatment of relapses triggered by virus infections in multiple sclerosis.

137

A NOVEL METHOD TO ESTABLISH CHRONIC RELAPSING EXPERIMENTAL AUTOIMMUNE ENCEPHALOMYELITIS IN SJL MICE

J. Yang*, V. Hukkanen and R. Seljelid.
*Department of Experimental Pathology, Institute of Medical Biology, University of Tromsø, Tromsø, Norway and Department of Virology, University of Turku, Turku, Finland
Fax +47-776-45400

Six to 8 weeks old female SJL/J mice were given a priming injection of neuroantigen and mycobacterial components in saline solution, followed by a standard EAE induction injection using neuroantigen and Freund's complete adjuvant two months later. In contrast to acute EAE, an early onset of the disease with slow recovery ensued. The majority of mice survived the first attack of EAE and the disease became chronic thereafter, with relapsing-remitting episodes. The various stages of the disease were found to be dependent on the doses of neuroantigen and anatomical sites of injection. Histology examination shows perivascular mononuclear infiltration and demyelination in the brain.The clinical course, as well as the histology resembles human multiple sclerosis.

138 LINOMIDE SUPPRESSES EAMG AND DOWN-REGULATES ACHR-INDUCED TH1 AND TH2 CYTOKINES

L-Y.Yu, F-D.Shi, G-X.Zhang, and H.Link. Division of Neurology, Huddinge Hospital, S-141 86 Huddinge, Sweden. Fax +46-8-7744822

Suppressive effect of the synthetic immunomodulatory drug Linomide (LS-2616) has been shown in some autoimmune diseases, including experimental autoimmune myasthenia gravis (EAMG), a model for human myasthenia gravis (MG). To define the mechanism underlying the suppression of EAMG, we injected linomide s.c at different doses to Lewis rats immunized by Torpedo AChR + FCA, and investigated AChR-specific T and B cell responses and the levels of AChR-induced cytokine mRNA expressing cells. Both 16 and 160, but not 1.6, mg/kg/day of linomide effectively suppress clinical muscle weakness, accompanied by decreased serum anti-AChR antibody levels, numbers of AChR-specific IgG antibody secreting cells, AChR-reactive IFN-γ secreting cells and lymphocyte proliferation to AChR. Further, linomide suppress not only Th1 cytokines IFN-γ and TNF-α, but also Th2 cytokines IL-4 and IL-10, while detecting their mRNA expressing cells by in situ hybridization. We conclude that, besides its affecting on NK cells, linomide suppresses EAMG also by downregulating Th1 and Th2 cytokines, which are important for the production of anti-AChR antibodies.

WORKSHOP 8. (ABSTRACTS 139–163) CLINICAL AND THERAPEUTIC IMMUNOLOGY

139 AUTOIMMUNE T AND B CELLS ARE AUGMENTED IN NEWBORN AND PREGNANT RATS

G-X.Zhang, B-G.Xiao, C-G.Ma, J.Link, T.Olsson and H.Link. Division of Neurology, Huddinge Hospital, S-141 86 Huddinge, Sweden. FAX +46-8-7744822.

Immunological changes in both mother and fetus during normal pregnancy are different from those in normal adult in several aspects. These changes may be related to the conceptus protection during pregnancy and the form of immune pattern of fetus in the future. To examine the occurrence of autoimmunity in neonates and during pregnancy, cell suspensions from spleen and thymus of newborn rats and peripheral blood from pregnant rats were examined for T and B cell responses to acetylcholine receptor (AChR) and myelin basic protein (MBP) which are important autoantigens in myasthenia gravis and multiple sclerosis, respectively. Compared to spleens from adult rats, neonate spleens contained higher numbers of AChR- and MBP-reactive interferon-γ secreting T cells and anti-AChR and anti-MBP antibody secreting cells. In thymus, no differences were found between neonate and adult rats. Pregnant rats had also elevated numbers of AChR- and MBP-specific T and B cells in blood. Both the neonate state and pregnancy are associated with physiologically augmented T and B cell autoreactivities with specificities observed in diseases with autoimmune background.

STIC-ILL

From: Gambel, Phillip
Sent: Tuesday, July 23, 2002 4:00 PM
To: STIC-ILL
Subject: refernces of recrod in ussn 09 / 010377 rubin encephalitis

stic

please provide the following references to

phillip gambel
art unit 1644
308-3997

1644 mailbox 9E12

MIC
RC321.A67

1) sanders et al. archives of neurology 53 : 125- 133 (1996)

2) editorial archives of neurology 53 : 123- 124 (1996)

3) soilo-hanninen et al. scand. j. immunol. 43 : 727 - ? (1996)

4) soilo-hanninen et al. j. neuroimmunol. 72 : 95 - 105 (1997)

5) planz et al. j. virol. 69 : 896 - 903 (1995)

thanx

ORIGINAL CONTRIBUTION

Herpes Simplex Virus in Postmortem Multiple Sclerosis Brain Tissue

Virginia J. Sanders, PhD; Aimee E. Waddell; Stephen L. Felisan; Ximing Li, MD; Andrew J. Conrad, PhD; Wallace W. Tourtellotte, MD, PhD

Background: Herpes simplex virus (HSV) is a common neurotropic virus that is capable of long latencies. It can cause focal demyelination in animals.

Objective: To test for the presence of HSV-1 and -2 in postmortem brain samples from patients with multiple sclerosis (MS) and controls using polymerase chain reaction and Southern blot hybridization.

Methods: Dissected plaque tissue classified as active or inactive and unaffected white matter (WM) and gray matter (GM) from 37 cases of MS were screened for HSV using polymerase chain reaction and Southern blot hybridization. White matter and GM from 22 cases of Alzheimer's disease, 17 cases of Parkinson's disease, and 22 cases without neurologic disease served as controls.

Results: Forty-six percent (17/37) of the MS cases and 28% (17/61) of the control cases had samples that were positive for HSV (P=.11). Forty-one percent (9/22) of active plaques and 20% (6/30) of inactive plaques were positive for HSV. Twenty-four percent (9/37) and 14% (5/37) of MS cases and 23% (14/61) and 13% (8/61) of non-MS cases had HSV in WM and GM, respectively. No significant differences were found among all subgroups (P=.10).

Conclusions: Herpes simplex virus was present in more MS cases than control cases and in more active plaques than inactive plaques. The presence of HSV in WM and GM in cases of MS as well as in control cases makes an etiologic association to the MS disease process uncertain, but cellular localization of HSV and its relationship to oligodendrocytes and latency may reveal such an association in future studies.

(Arch Neurol. 1996;53:125-133)

From the Brain Research Institute, University of California, Los Angeles (Drs Sanders and Conrad); the Department of Neurology, University of California, Los Angeles, School of Medicine (Ms Waddell, Mr Felisan, and Drs Sanders, Li, Tourtellotte, and Conrad); and the Neurology and Research Services, West Los Angeles Veterans Affairs Medical Center (Drs Sanders, Li, Conrad, and Tourtellotte, Ms Waddell, and Mr Felisan).

MULTIPLE sclerosis (MS) is characterized by multifocal lesions of demyelination and inflammation.[1] Its cause remains unknown. The theory addressed in this report proposes that a virus persistent in the central nervous system (CNS) is responsible for MS; a candidate could be herpes simplex virus 1 and 2 (hereafter referred to simply as *HSV*).

Herpes simplex virus is a common human pathogen; 70% to 80% of the population have antibodies to HSV.[2] The hallmark characteristic of the herpesviruses is their capability for latency. The virus remains latent in the neurons of the trigeminal or sacral ganglia until reactivation, which results in centrifugal spread to the site of infection and possible spread into the CNS.[3] Polymerase chain reaction (PCR) detected HSV in the trigeminal ganglia in 72% of a postmortem population; all of the sampled population older than 60 years were infected.[4] The virus has also been detected in 35% of nonneurologically diseased brains.[5]

Herpes simplex virus can induce multifocal demyelination in experimental animals. Inoculation with HSV-1 results in primary demyelination and inflammatory infiltrates.[6,7] Both active and inactive plaques are present in mice for prolonged periods; viral antigen and viral DNA are not present after 21 days, although active plaques can still be seen as long as 8 weeks after inoculation.[8] Having crossed the blood-brain barrier, the virus can spread easily through the CNS.[5,6,9,10]

Patients with MS have immune abnormalities suggestive of herpes infection. The elevated intrathecal IgG synthesis rate and the presence of unique CSF IgG oligoclonal bands in patients with MS are similar to those in patients who have recovered from herpes simplex encephalitis, who may also demonstrate viral an-

See Materials and Methods on next page

MATERIALS AND METHODS

BRAIN SAMPLES

One hundred twenty-six postmortem brain samples from 37 patients with MS were examined. Disease duration ranged from 4 to 47 years. A total of 204 postmortem samples obtained from 22 subjects with Alzheimer's disease, 17 subjects with Parkinson's disease, and 22 subjects without neurologic disease were used as controls (**Table 1** and **Table 2**).

TISSUE PREPARATION

All postmortem brains were received on ice and immediately cut into 5-mm-thick coronal sections; a clean knife was used for each slice. Any blood remaining on the coronal section was wiped off. Sections were sealed in plastic bags and flash frozen between aluminum plates in liquid nitrogen. All specimens were stored at −70°C.[13]

Brain areas were dissected with separate disposable microtome blades. White matter tissue blocks did not contain any GM and vice versa. Blocks that contained plaques did have, by necessity, some periplaque WM. Any gross-appearing GM was trimmed away. To prevent any possible contamination of blocked tissue from previously amplified PCR products and other foreign substances, approximately 100 μm of each block was cryosectioned and discarded before sections were cut for PCR. A separate disposable microtome blade was used for each section. The subsequent sections were used for routine staining (hematoxylin-eosin and oil red O) and for immunocytochemical staining for the major histocompatibility complex class II immunologic marker HLA-DR. Each tissue sample was characterized histologically by a four-scale classification as follows[1]:

Type 1. Earliest lesion in which activated microglia are responding to initial events of the disease process. There is no evidence of myelin breakdown. Some of these regions appear similar to microglial nodules.

Type 2. Active lesion in which microglia at the edge of the plaque are immunologically activated. Macrophages toward the center of the plaque have converted myelin debris to neutral lipid (**Figure 1** and **Figure 2**).

Type 3. Modestly active lesion in which there is a distinct edge of activated microglia and macrophages. The center of the lesion is completely demyelinated.

Type 4. Least active or completely inactive lesion in which activated microglia and macrophages may be present but no neutral lipid or myelin debris remains.

In this study, we compared type 2 plaques with type 4 plaques; in further studies, we will screen other plaque types. There were 22 type 2 plaques, 30 type 4 plaques, and 37 normal-appearing WM and GM samples each. Seven cases consisted of a type 2 plaque, WM, and GM; 15 cases were composed of a type 4 plaque, WM, and GM; and 15 others were made up of all tissue types. Control tissue consisted of periventricular WM and cortical GM from subjects with (1) Alzheimer's disease, (2) Parkinson's disease, and (3) no neurologic disease. A sample containing both GM and WM from the temporal lobe of a subject with herpes simplex encephalitis was used as a positive control.

NUCLEIC ACID EXTRACTION AND PURIFICATION

Cryosections from each block were placed in 100-μL ribonuclease-free, deoxyribonuclease-free deionized water and stored at −70°C. Nucleic acids were extracted by guanidinium isothiocyanate-alkaline phenol–chloroform,[14] followed by ethanol precipitation with glycogen as a carrier.

PRIMERS

The oligonucleotide primer sequences were 5′TTGAAGCGGTCGGCGGCGTA-3′ and 5′GCATCGTCGAGGAGGTGGA-3′(Bioserve Biotechnologies, Laurel, Md), giving a 148–base pair amplification product. This primer set is from a highly conserved region of the polymerase gene[15] and gives a product specific for both HSV-1 and HSV-2. Primers were checked for primer-dimer formation, hairpin formation, and mispriming sites with a 4.0 primer selection software program (Oligo, National Biosciences, Plymouth, Minn). Cross-reactivity with human genomic sequences was checked by means of a BLAST (Basic Local Alignment Search Tool) search. There was no cross-reactivity of these primers with Epstein-Barr virus, cytomegalovirus, varicella-zoster virus, or human herpesvirus 6 as determined by our using each of these viruses as template for PCR amplification and Southern blot detection and not obtaining a positive signal for any of the other viruses (data not shown).

AMPLIFICATION AND SOUTHERN BLOT DETECTION

Polymerase chain reaction amplification was carried out with the use of heat-stable *Taq* DNA polymerase in a total reaction volume of 100 μL containing between 0.6 and 1.0 μg of the extracted nucleic acid as a template. The optimized reaction conditions used consisted of 200-μmol/L each deoxynucleotide triphosphate (2′-deoxyadenosine-

tibody (both specific and nonspecific) intrathecally up to 11 years after infection.[11] A dissociation of lymphocytic response to HSV has been reported in patients with

For editorial comment see page 123

MS. Isolated MS lymphocytes were not stimulated to an activated state when challenged by HSV; whereas other viruses did induce activation of MS lymphocytes equivalent to that found in controls.[12]

We propose that the demyelination seen in MS is due to different causes in different cases. A case-by-case analysis resulting in a subset of cases in which HSV is detected in active plaques would support this proposal. It is not proof of cause and effect, but rather a necessary first step. In our study, dissected MS plaques were histologically and immunocytochemically characterized for myelin debris and immunologic activity. Samples of normal-appearing white matter (WM) and gray matter (GM) from the same subjects with MS were also studied to serve as a type of control. Adjacent sections were examined by PCR and Southern blot hybridization to determine the incidence of HSV. Samples of normal-appearing WM and GM from subjects without MS were also studied to serve as a further control.

5′-triphosphate, 2′-deoxy-cytidine-5′-triphosphate, 2′-deoxy-guanosine-5′-triphosphate, and 2′-deoxy-thymidine-5′-triphosphate), 100 pmol/L of each primer, 0.01% acetylated bovine serum albumin, 1.5-mmol/L magnesium chloride, 50-mmol/L potassium chloride, 10-mmol/L TRIS (pH, 9.0), and 0.1% Triton X-100. One unit of *Taq* polymerase (Promega, Madison, Wis) was added in a modified "hot start" procedure using presized sterile wax beads (AmpliWax, Perkin-Elmer Corp, Norwalk, Conn). The reagents were heated and the *Taq* was added during the first thermocycling step. The thermocycling parameters were 60 seconds at 95°C, 90 seconds at 60°C, and 90 seconds at 72°C, and amplification was performed for 40 cycles. Thermocycling was followed by a 10-minute final extension incubation at 72°C. Each specimen was run in triplicate within each thermocycling batch.

After thermocycling, 10% of each PCR-amplified product was run on a 1.0% agarose gel, partially depurinated, and suction blotted onto a nylon membrane (Stratagene, La Jolla, Calif). The membranes were probed with a digoxigenin-labeled oligonucleotide fragment specific for the PCR-amplified product using the methods and reagents outlined in the manufacturer's kit (Genius, Boehringer-Mannheim Corp, Indianapolis, Ind). After probe hybridization, the membranes were developed with alkaline phosphatase–conjugated, digoxigenin-specific antibody. Colorimetric detection was carried out with 4-nitroblue tetrazolium chloride and 5-bromo-4-chloro-indolyl-phosphate (Boehringer-Mannheim Corp). The position of probe-detected bands compared with molecular-weight markers (molecular-weight marker VI, Boehringer-Mannheim Corp) were consistent with the expected amplification product size (**Figure 3**).

Semiquantitation, when performed, was as follows: the membranes were digitized on a scanner (model IIc, Hewlett-Packard Co, Palo Alto, Calif) at 300 dots per inch, 256-level gray scale (eight-bit), 100% size. The image-processing software (Image 1.52, public domain software written by Wayne Rasband of the National Institutes of Health, Bethesda, Md) was used to identify and outline bands (image particles) and to quantify band area and mean band density. The product of band area and mean density gives a reliable indication of the amount of "blackness" present in a band, and was compared with a derived standard curve to give a numerical value of the copy number for each band.[16]

To minimize tissue contamination, tissue preparation, nucleic acid extraction, PCR reagent preparation, and the amplification and detection procedures were performed in three separate buildings. Standard procedure dictated the use of disposable gowns and hair and shoe covers for all laboratory personnel before they entered the tissue preparation laboratory. All laboratories were irradiated daily by mercury UV lamps. Laboratory technicians were assigned to separate duties. All pipette tips, tubes, and gels used for analyzing PCR products were discarded in a waste receptacle containing a 0.1-mol/L hydrochloride solution; similarly, all nonporous surfaces within the laboratories were wiped down with diluted hydrochloride to minimize carryover into other rooms.

POSITIVE AND NEGATIVE REACTION CONTROL DESIGN

To identify and minimize the effect of false positives or false negatives, we instituted a number of quality controls on each of our experiments. To identify false-positive results (1) 25% reagent blank controls (double-distilled water was added instead of sample) were included in each PCR thermocycling batch; (2) 10% of all reaction tubes were true-negative controls (double-distilled water was run through the entire nucleic acid extraction procedure); (3) each specimen was run in triplicate (a specimen exhibiting only one positive was suspected of being a false positive and was rerun); and (4) 40-tube PCR batches containing 36 reagent blanks and one positive control serial dilution served as a redundant check on our contamination-prevention efforts.

The following steps were taken to ensure that each PCR batch exhibited proper sensitivity:

1. A serial dilution of HSV-1 strain DNA extract of known concentration (Catalog No. 08-705-000, Advanced Biotechnologies Inc, Columbia, Md) representing one to 1000 copies per reaction was added to each PCR batch as a sensitivity control (Figure 3).

2. Nucleic acid extracted from temporal lobe tissue from a case of herpes simplex encephalitis was used as an overall positive control for each experiment.

3. Data was obtained only from (*a*) membranes that exhibited a PCR sensitivity of at least 10 copies per reaction, (*b*) all positive controls exhibiting a strong specific band, and (*c*) every one of the negative control and reagent blank lanes exhibiting no specific bands. All tissue specimens were coded at the time of specimen preparation and remained coded until after all membranes in the study were developed.

STATISTICS

The χ^2 statistic (with continuity correction as needed) was used to compare frequencies of positive signals among groups with a cutoff *P* value of .05.[17]

RESULTS

REPRODUCIBILITY AND ACCURACY CHECKS

1. The stability of viral DNA against autolytic enzymes was investigated by means of a 30-cycle PCR experiment performed on cryosections from a case of herpes simplex encephalitis stored at 4°C, 25°C, and 37°C for 1, 2, and 7 days each. All groups were run in quadruplicate. Densitometric analysis of Southern-blotted amplification products showed no significant differences among the groups at different autolysis times and different temperatures, suggesting that there was no effect of autolysis time on viral DNA integrity under these conditions (**Figure 4**).

2. Variability of nucleic acid purification and recovery was tested by comparing the signal of three groups of samples of precisely equal starting material. Dilutions of a herpes simplex encephalitis tissue homogenate were extracted (1:1, 1:100, and 1:10 000), and the resulting amplified product signals were compared. There were 12 tubes per group. There was no significant difference among the tubes within each group, indicating that there was no systematic variability in nucleic acid purification and recovery (**Figure 5**).

Table 1. Information in Cases of Multiple Sclerosis (MS), Listed by Increasing Duration of Disease

HSB No.*	Age, y/ Sex	Disease Duration, y	Cause of Death	Autolysis, h
735	39/M	4	Pneumonia	6
894	38/M	5	Pneumonia	60
944	33/F	6	Septicemia	22.5
644	37/F	8	Cardiac arrest	11
793	58/F	8	Pneumonia	5
802	48/F	8	Pneumonia	10.5
573	50/F	9	Overdose/suicide	15
678	40/M	10	Cardiac arrest	5.5
536	31/M	11	Cardiac arrest	25
1864	37/F	11	Anoxia	12
1035	66/M	12	Pneumonia	10.5
511	40/M	13	Respiratory failure	12
1238	36/F	13	Gastrointestinal bleeding	19.5
1134	51/M	14	Septicemia	35
1862	69/M	14	Septicemia	9
2190	70/M	14	Respiratory failure	9
1011	44/M	16	Pneumonia	4.5
1337	59/F	16	MS	14
1291	44/F	19	Cardiac arrest	7
996	41/F	20	Fibrosarcoma	14
888	50/M	21	Pneumonia	8
1145	42/M	22	Anoxia	31.5
344	42/M	23	Pneumonia	6
845	45/M	23	Drowning	28
1588	46/F	23	Respiratory failure	24
1061	50/F	24	MS	12
934	50/F	25	Pneumonia	11.5
1174	65/M	27	Septicemia	12
640	51/M	28	Pneumonia	23
1446	51/F	29	Pneumonia	4.5
1270	67/F	30	Septicemia	23.5
1668	59/F	32	Septicemia	9.5
909	70/F	40	Undetermined	31
1088	64/F	40	Renal failure	11.5
579	61/M	41	Pneumonia	12
338	65/M	44	Pneumonia	6
1779	69/F	47	Lung cancer	6.5

*HSB indicates Human Specimen Bank.

3. Variability of amplification efficiency within a PCR experiment and between PCR experiments was examined. Intensity of sequence-specific Southern blot bands from seven serial dilutions of HSV-1 MacIntyre strain DNA extract (one to 1000 copies per reaction) from three different PCR runs was measured. The serial dilutions were plotted, and the equations of the resulting lines were determined. There were no differences among the determined line equations from different dilution series within a PCR experiment (**Figure 6**).

DETECTION OF HSV

Multiple Sclerosis

The overall incidence of cases that were positive for HSV within the entire MS group was 46% (17/37) (**Table 3**): 41% (9/22) of the type 2 plaques, 20% (6/30) of the type 4 plaques, and 24% (9/37) and 14% (5/37) of normal-appearing WM and GM, respectively, were positive for HSV. There was no significant difference among these frequencies ($P=.11$).

Case-by-case analysis of the patterns of virus distribution showed that 32% (12/37) fulfilled the criteria for presence of virus in some meaningful combination (**Table 4**). Three cases had virus only in type 2 plaques; three had virus in type 2 and type 4 plaques; two had virus in type 2 and type 4 plaques and in normal-appearing WM; one had virus in all sample types; one had virus in type 2 plaques and in normal-appearing WM and GM; one had virus in type 2 plaques and in normal-appearing WM; and one had virus present in type 2 plaques and in normal-appearing GM. There were five other cases that had a variable distribution of positive signals, none of which were found in type 2 plaques.

Controls

Seventeen (28%) of 61 control cases were positive for HSV (**Table 5**): six (27%) of the 22 cases without neurologic disease, five (23%) of the 22 cases of Alzheimer's disease, and six (35%) of the 17 cases of Parkinson's disease. There were no significant differences among control subgroups. Among the control cases, HSV was present in 23% (14/61) of the cases in which WM was sampled and in 13% (8/61) of those in which GM was sampled. There was no significant difference between the frequency of cases with positive WM samples and cases with positive GM samples.

MS vs non-MS Controls

In the MS group, 46% of the samples were positive for HSV (Table 3); 28% of all the samples in the non-MS control group were positive for HSV (Table 5). There was no significant difference between these groups ($P=.11$). In the MS group, HSV was found in 24% and 14% of the WM and GM samples, respectively, and in the non-MS group, it was found in 23% and 13% of the samples. There was no significant difference between these groups either ($P=.10$).

Because of inherent differences in tissue type (plaque, WM, and GM) and size of sections affecting cell number per section and amount of DNA present, the association between quantity of DNA and frequency of HSV positivity was statistically analyzed. There was no statistically significant difference in the quantity of DNA and the incidence of positive signals (data not shown; $P=.20$). Therefore, the positive signals were not simply the result of greater DNA concentrations being used as template.

COMMENT

Our laboratory has taken precautions to avoid the inherent pitfalls associated with the extreme sensitivity of the PCR procedure. We have demonstrated that our detection method is reliably sensitive for detecting between one and 10 virus copies per reaction. It has been

Table 2. Control Case Information, Sorted by Diagnosis*

HSB No.	Age, y/ Sex	Diagnosis	Disease Duration, y	Cause of Death	Autolysis, h
648	52/F	NND	NA	Suicide	20
1264	45/M	NND	4	Pneumonia/lung cancer	15
1289	74/M	NND	NA	Cardiorespiratory failure	8.5
1502	79/M	NND	NA	Cardiorespiratory failure	19.5
1508	78/F	NND	NA	Cardiorespiratory failure	7
1539	68/M	NND	1	Metastatic cancer	16.5
1640	66/M	NND	NA	Pneumonia	15.5
1645	70/F	NND	NA	Cardiorespiratory failure	8
1732	72/M	NND	NA	Cardiorespiratory failure	19.5
1736	76/M	NND	NA	Cardiorespiratory failure	17.5
1768	71/M	NND	NA	Pulmonary embolism	25
1775	69/M	NND	NA	Cardiorespiratory failure	17
1797	80/M	NND	NA	Cardiorespiratory failure	26.5
1818	59/M	NND	NA	Cardiorespiratory failure	15
1846	73/M	NND	NA	Pneumonia	26.5
1903	70/M	NND	NA	Cardiorespiratory failure	13
1933	48/M	NND	NA	Cardiorespiratory failure	15
2104	71/M	NND	NA	Pneumonia	25.5
2181	68/M	NND	Undetermined	Lung cancer	7
2187	55/M	NND	NA	Cardiorespiratory failure	24.25
2255	73/M	NND	NA	Cardiorespiratory failure	23.5
2308	68/M	NND	NA	Myocardial infarction	20
1702	76/F	AD	15	Cardiorespiratory failure	5.5
1723	77/F	AD	Undetermined	Undetermined	12
1733	80/M	AD	6	Cardiorespiratory failure	19
1739	84/M	AD	6	Pneumonia	8
1746	75/M	AD	6	Cardiorespiratory failure	5.5
1801	75/F	AD	4	Pneumonia	19
1972	79/F	AD	Undetermined	AD	6.5
1979	83/M	AD	6	Pneumonia	13
1988	87/F	AD	6	AD	4.5
2005	84/M	AD	8	Metastatic colon cancer	8.5
2078	86/F	AD	9	Cardiorespiratory failure	12.5
2080	77/F	AD	Undetermined	Undetermined	8.5
2162	75/M	AD	12	Cerebral infarct	5
2166	84/F	AD	17	Pneumonia	14.5
2173	79/F	AD	3	Pulmonary embolism	5.5
2175	83/M	AD	Undetermined	Undetermined	7.5
2182	92/F	AD	8	Cardiorespiratory failure	10.5
2186	83/F	AD	8	Undetermined	9
2188	80/M	AD	3	Cardiorespiratory failure	20.5
2195	80/F	AD	5	Undetermined	8.25
2196	87/F	AD	5	AD	7
2177	72/M	AD	6	Cardiorespiratory failure	9
1259	79/M	PD	Undetermined	Pneumonia	21.5
1303	78/M	PD	3	Cardiorespiratory failure	8.5
1315	74/M	PD	13	Cardiorespiratory failure	10
1567	76/M	PD	Undetermined	Undetermined	19
1593	79/M	PD	17	Cardiorespiratory failure	5
1613	85/M	PD	23	Cerebral infarct	7.5
1658	78/M	PD	5	Urosepsis	21
1746	78/M	PD	12	Undetermined	5.5
1747	75/M	PD	Undetermined	Renal failure	5
1767	72/M	PD	27	Cardiorespiratory failure	5.5
1810	65/M	PD	19	Multiple myeloma	7
1889	76/M	PD	18	Adenocarcinoma	15.5
1971	80/M	PD	5	Cardiorespiratory failure	9
2004	81/M	PD	10	Undetermined	7
2163	83/F	PD	11	Cardiorespiratory failure	9
2262	83/M	PD	Undetermined	Cardiorespiratory failure	15
2290	75/M	PD	9	Cerebral infarct	12

HSB indicates Human Specimen Bank; NND, nonneurologic disease; AD, Alzheimer's disease; PD, Parkinson's disease; and NA, not applicable.

Figure 1. *Type 2 plaque. Large focal plaque filled with immunologically activated macrophages. Activated microglia form distinct rim of this plaque (monoclonal antibody to HLA-DR, original magnification ×40).*

Figure 2. *Type 2 plaque. Sequential section of the plaque seen in Figure 1. Large focal plaque composed of lipid-filled macrophages (oil red O, original magnification ×40).*

established that the viral DNA does not degrade significantly and that there is relatively little variability in nucleic acid extraction and amplification efficiency between identical specimens, suggesting that our PCR amplification is not overshadowed by random error. Hence, our methodology is sensitive, specific, reproducible, and without contamination.

MULTIPLE SCLEROSIS

We found HSV in a subset of CNS samples from both patients with MS and control patients. Seventeen (46%) of 37 cases of MS had samples that were positive for HSV. These data, analyzed on a case-by-case basis, are in keeping with our idea that there is more than one cause of MS. For a given virus to be involved in the pathogenesis of MS, it must be present in plaque tissue. It is an expected result that individual cases may have dissimilar patterns of distribution of a candidate virus in different tissue types (Table 4). Our hypothesis predicts that HSV or other possible causative agents will be present and active in type 2 plaques, but it is also possible that latent virus will be present. In distribution patterns II, III, and IV, it is possible that some active virus will be found in type 4 plaques, but the majority will be latent. In the other distribution patterns, the virus should be in a latent phase in normal-appearing WM and GM. Future experiments will determine the latency state of the virus in each of the blocks studied.

Within the entire MS group, 41% of the active type 2 plaques were positive for HSV, whereas only 20% of the type 4 and 25% and 14% of the normal-appearing WM and GM tissue samples, respectively, were positive for HSV. Our results suggested a trend but did not show any significant differences. Perhaps the virus was not completely eradicated from the inactive lesions or that it is in a latent form in these plaques and in normal-appearing WM and GM.

Until infected cells are identified, it is not possible to determine whether the virus is a causative agent, is merely present in a latent form, or is a consequence of the immunologic activation associated with active demyelination. The higher prevalence of virus in active type 2 plaques may be attributable to the inflammatory response occurring in the lesion site, but the 14 type 2 plaques that were negative for HSV (Table 3) argue against this explanation. These actively demyelinating plaques are without virus but contain inflammatory infiltrates simi-

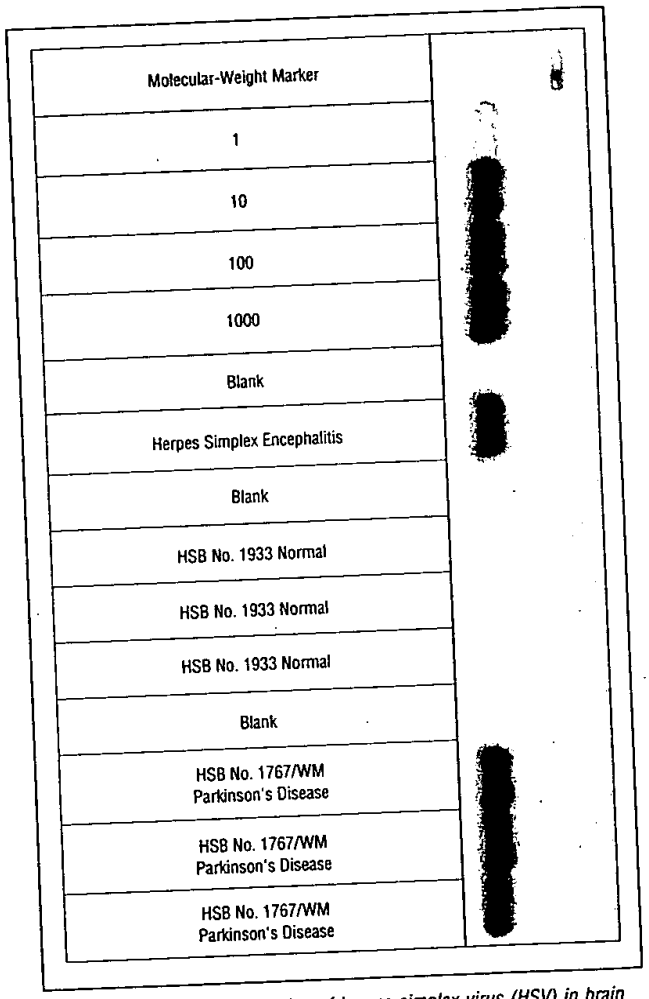

Figure 3. *Southern blot detection of herpes simplex virus (HSV) in brain samples. Lane 1, molecular-weight marker; lanes 2 through 5, HSV serial dilution (one to 1000 copies per microliter); lanes 6, 8, and 12, negative controls; lane 7, temporal lobe from a case of herpes simplex encephalitis; and lanes 9 through 11 and 13 through 15, white matter (WM) samples from a case without neurologic disease (Human Specimen Bank [HSB] No. 1933) and a case of Parkinson's disease (HSB No. 1767).*

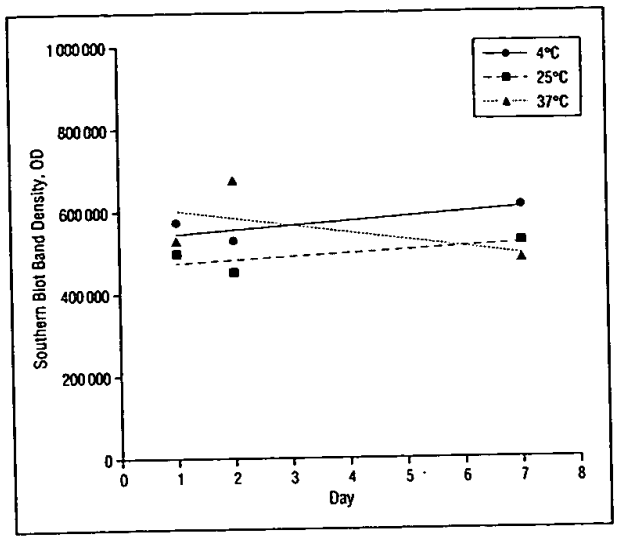

Figure 4. *Effect of autolysis time (1, 2, or 7 days) and different temperatures (4°C, 25°C, or 37°C) on integrity of viral DNA from herpes simplex encephalitis brain tissue as determined by semiquantitative polymerase chain reaction and Southern blot hybridization. OD indicates optical density of membrane band.*

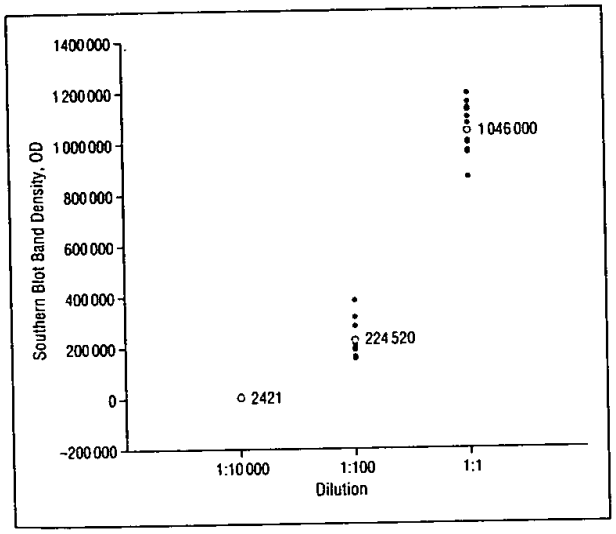

Figure 5. *Variability of nucleic acid extraction and recovery procedure. Comparison of three groups (N=12) of precisely equal starting material (1:1, 1:100, and 1:10 000 dilutions of herpes simplex encephalitis tissue homogenate) as determined by semiquantitative polymerase chain reaction and Southern blot hybridization. OD indicates optical density of membrane band.*

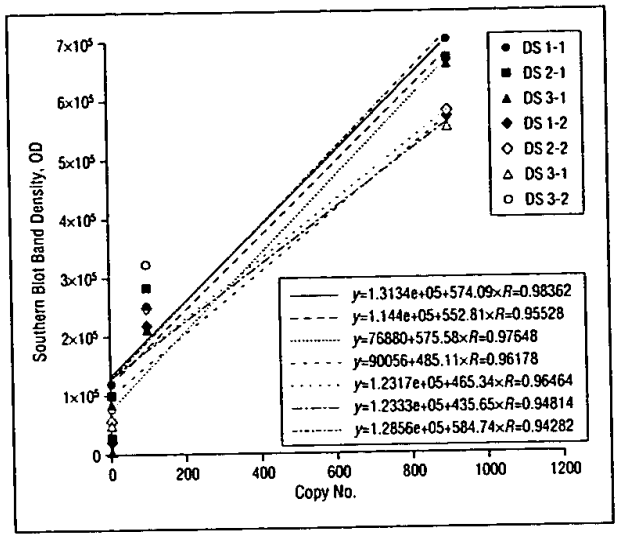

Figure 6. *Variability of amplification efficiency within a polymerase chain reaction (PCR) experiment and between PCR experiments. Comparison of serial dilutions of herpes simplex virus 1 DNA extract (one to 1000 copies per reaction) from three different PCR runs. The serial dilutions were plotted, and the equations of the resulting lines were determined. DS indicates dilution series, denoted by PCR run number followed by series number; OD, optical density of membrane band. Note: Slope (R) and intercept (y) are similar for each equation derived from the line plotted for each dilution series.*

Table 3. Cases of Multiple Sclerosis (MS) Positive for Herpes Simplex Virus (HSV)*

HSB No.	Disease Duration, y	Type 2 Plaque	Type 4 Plaque	WM	GM
2190	14	Positive	Negative	Negative	Negative
344	23	Positive	Negative	Negative	Negative
934	25	Positive	NA	Negative	Negative
678	10	Positive	Positive	Negative	Negative
1588	23	NA	Positive	Negative	Negative
1174	27	NA	Positive	Negative	Negative
944	6	Positive	NA	Positive	Negative
1270	30	NA	Positve	Positive	Negative
1238	13	Positive	Positive	Positive	Positive
802	8	Positive	Negative	Negative	Positive
1864	11	Negative	Negative	Positive	Negative
1134	14	NA	Negative	Positive	Negative
888	21	Positive	Negative	Positive	Positive
845	23	Negative	Positive	Negative	Positive
640	28	Positive	Negative	Positive	Negative
909	40	NA	Negative	Positive	Positive
1779	47	NA	Negative	Positive	Negative
Total Positive, No. (%)	...	**9/22 (41)**	**6/30 (20)**	**9/37 (24)**	**5/37 (14)**

**A total of 17 (46%) of the 37 cases of MS were positive for HSV. HSB indicates Human Specimen Bank; WM, white matter; GM, gray matter; and NA, not applicable.*

lar to those in plaques with virus. This situation implies that the inflammation of MS per se does not bring in HSV-infected cells from the blood. These type 2 plaques without HSV could be attributable to another cause. Nevertheless, if HSV is related to the MS disease process, it is reasonable that active virus would be found at the highest frequency in areas of immunologic activity and recent destruction of myelin.

To our knowledge, it has not been reported that HSV is found more frequently in WM than GM. In our study, the careful dissection of pure WM or GM reduced the possibility of contamination. Perhaps the sensitivity of PCR permitted the detection of low levels of HSV (either active or latent) in neurons that are located in the WM or in nonneuronal cells. Astrocytes and oligodendrocytes may be infected by HSV[18-20]; other nonneuronal cells (eg, macrophages, microglia, endothelial cells, and intravascular leukocytes) may contribute to the positive signal. It is also possible that the virus is in the axon of its infected neuron located in nearby GM. On the other hand, the infected normal-appearing WM could be prelesional, where

Table 4. Patterns of Virus Distribution in Postmortem Multiple Sclerosis Brain Tissue*

Pattern	Type 2 Plaque	Type 4 Plaque	NAWM	NAGM	HSB Nos.
I	Present	Not present	Not present	Not present	344, 934, 2190
II	Present or NA	Present	Not present	Not present	678, 1174, 1588
III	Present or NA	Present	Present	Not present	944, 1270
IV	Present or NA	Present	Present	Present	1238
V	Present	Not present	Present	Present	888
VI	Present	Not present	Present	Not present	640
VII	Present	Not present	Not present	Present	802

**NAWM indicates normal-appearing white matter; NAGM, normal-appearing gray matter; HSB, Human Specimen Bank; and NA, not available.*

viral load is either in a latent stage or active but too low to cause distinct tissue damage.

The positive results in our cases of MS are in contrast to those of Nicoll et al,[21] who reported that only one of the samples obtained from 23 patients with MS was positive for HSV. They used formalin-fixed, paraffin-embedded tissue and detected the amplified product with ethidium bromide, which is less sensitive than Southern blot hybridization. These differences in methodology could explain the different results.

CONTROLS

Herpes simplex virus was found in 27% of the patients without neurologic disease, in 23% of the patients with Alzheimer's disease, and in 35% of the patients with Parkinson' disease. The presence of HSV in the CNS of such a high percentage of cases is not a surprise owing to the ubiquitous and neurotropic nature of the virus. Similarly, it is not unreasonable to find HSV in tissue with no obvious disease, as is the case when the trigeminal ganglia are infected with latent virus.

Our results differ from those of other studies that have examined brain tissue for the presence of HSV using PCR. Alexander et al[22] did not find HSV in any samples of temporal lobe tissue obtained in schizophrenic, nonschizophrenic suicide, or normal control cases. In contrast, Jamieson et al[23] found HSV in frontal, temporal, and hippocampal tissue samples in all eight cases of AD and in six normal control cases. The small size of these studies could explain the conflicting results.

Our study expands on the work by Baringer and Pisani,[5] who reported a baseline frequency rate of HSV in 35% of nonneurologically diseased brains. The authors confined their search to the trigeminal ganglia, olfactory bulbs, medulla, pons, hippocampus, amygdala, gyrus rectus, calcarine cortex, and cerebellum. All the samples contained both GM and WM. Herpes simplex virus was most frequently detected in the pons, medulla, and olfactory bulbs. While an association of HSV with neurologic disease is not refuted by the authors, they caution other researchers to be conservative about interpretation of results based on frequency rates.

Our study, because of the different focus, examined cortical GM and WM primarily from the corona radiata; to our knowledge, this is the first study to discriminate between tissue types (plaque type as well as WM and GM). Despite the differences in samples examined, our results are in accord with those of Baringer and Pisani.[5]

Table 5. Control Cases Positive for Herpes Simplex Virus*

HSB No.	Diagnosis	White Matter	Gray Matter
1645	NND	Positive	Negative
1736	NND	Positive	Negative
1768	NND	Negative	Positive
1818	NND	Positive	Negative
1903	NND	Positive	Negative
2308	NND	NS	Positive
1702	AD	Negative	Positive
1723	AD	Positive	Negative
1801	AD	Positive	Positive
1979	AD	Positive	Positive
2188	AD	Positive	Negative
1315	PD	Positive	Negative
1658	PD	Positive	Positive
1746	PD	Positive	Negative
1747	PD	Positive	Negative
1767	PD	Positive	Negative
1810	PD	Positive	Positive

**NND indicates nonneurologic disease; AD, Alzheimer's disease; PD, Parkinson's disease; and NS, not sampled. Six (27%) of 22 NND cases, five (23%) of 22 AD cases, and six (35%) of 17 PD cases were positive for HSV (total, 17 [28%] of 61).*

MS vs CONTROL CASES

Herpes simplex virus was found slightly more often in cases of MS than in control cases, although the difference was not statistically significant. It would be premature to explain this difference as proof of causation. Other explanations are compelling as well. Patients with MS are usually treated with steroids or other immunosuppressants. The immunosuppression occurring in the patients because of the medications could allow for the reactivation of the virus and travel across the blood-brain barrier. The virus may enter the brain through infected macrophages or lymphocytes that are sometimes seen in the perivascular space of grossly normal-appearing tissue. Another possibility is that because of the different cellular milieu, virus is technically more easily identified in type 2 plaques and WM than in type 4 plaques and GM.

The significance of our results to MS is yet to be determined, especially in view of the high frequency of virus found in non-MS cases. However, this study is our first step in elucidating the role of HSV in the pathogenesis of MS. Multiple sclerosis may have many different causes, all resulting in primary demyelination. Our data support this notion, since 59% of type 2 plaques did not contain HSV, in contrast to 41% that did. A long-term goal of our laboratory is to establish which cell or cells may be harboring a latent or active virus in the samples positive for HSV. Will oligodendrocytes in active plaques contain HSV that is expressing proteins, in contrast to inactive and normal-appearing WM and GM in which HSV is latent?

Accepted for publication October 5, 1995.

This study was supported in part by grant RG 929-L-35 from the National Multiple Sclerosis Society Human Neurospecimen Bank and by medical research funds from the Department of Veterans Affairs.

We thank the many individuals who work in the National Neurological Research Specimen Bank, especially Iris Rosario, RN, James Riehl, MT(ASCP), Peter Chun, and Randall Warwick. We also thank Diane Guntrip for administrative assistance, and Karl Syndulko, PhD, for assistance with statistical analysis.

Reprint requests to Neurology Services (127A), West Los Angeles Veterans Affairs Medical Center, 11301 Wilshire Blvd, Los Angeles, CA, 90073 (Dr Tourtellotte).

REFERENCES

1. Sanders V, Conrad A, Tourtellotte WW. On classification of postmortem MS plaques for neuroscientists. *J Neuroimmunol.* 1993;46:207-214.
2. Whitley R. Herpes simplex virus. In: Fields B, Knipe D, eds. *Fields' Virology.* New York, NY: Raven Press; 1990:1843-1887.
3. McKendall RR. Herpes simplex. In: McKendall RR, ed. *Viral Disease.* Amsterdam, the Netherlands: Elsevier Science Publishers; 1989:207-227.
4. Liedtke W, Opalka B, Zimmerman CW, Lignitz E. Age distribution of latent herpes simplex virus 1 and varicella-zoster virus genome in human nervous tissue. *J Neurol Sci.* 1993;116:6-11.
5. Baringer JR, Pisani P. Herpes simplex virus genomes in human nervous system tissue analyzed by polymerase chain reaction. *Ann Neurol.* 1994;36:823-829.
6. Hill TJ. Herpesviruses in the central nervous system. In: Mims CA, Cuzner ML, Kelly RE, eds. *Viruses and Demyelinating Diseases.* Orlando, Fla: Academic Press Inc; 1983:23-45.
7. Kristensson K, Svennerholm B, Persson L. Latent herpes simplex virus trigeminal ganglionic infection in mice and demyelination in the central nervous system. *J Neurol Sci.*1979;43:253-264.
8. Kastrukoff LF, Lau AS, Leung GY, Walker D, Thomas EE. Herpes simplex virus type 1 (HSV-1)-induced multifocal central nervous system demyelination in mice. *J Neuropathol Exp Neurol.* 1992;51:432-439.
9. Esiri MM. Herpes simplex encephalitis: an immunohistological study of the distribution of viral antigen within the brain. *J Neurol Sci.* 1982;54:209-226.
10. Esiri M, Morris C, Millard P. Sensory and sympathetic ganglia in HIV-1 infection: immunocytochemical demonstration of HIV-1 viral antigens, increased MHC class II antigen expression and mild reactive inflammation. *J Neurol Sci.* 1993;114:178-186.
11. Riikonen R, Meurman O. Long-term persistence of intrathecal viral antibody responses in postinfectious diseases of the central nervous system and in Rett syndrome. *Neuropediatrics.*1989;20:215-219.
12. de Silva SM, McFarland HF. Multiple sclerosis patients have reduced HLA class II–restricted cytotoxic responses specific for both measles and herpes virus. *J Neuroimmunol.* 1991;35:219-226.
13. Tourtellotte WW, Rosario IP, Conrad A, Syndulko K. Neurospecimen banking 1961-1992. *J Neural Transm Suppl.* 1993;39:5-15.
14. Chomczynski P, Sacchi N. Single-step method of RNA isolation by acid guanidinium thiocyanate–phenol-chloroform extraction. *Anal Biochem.* 1987;162:156-159.
15. Rowley AH, Whitley RJ, Lakeman FD, Wolinsky SM. Rapid detection of herpes simplex virus DNA in cerebrospinal fluid of patients with herpes simplex encephalitis. *Lancet.* 1990;335:440-441.
16. Schmid P, Conrad A, Syndulko K, et al. Quantifying HIV-1 proviral DNA using the polymerase chain reaction on cerebrospinal fluid and blood of seropositive individuals with and without neurologic abnormalities. *J Acquir Immune Defic Syndr.* 1994;7:777-788.
17. Siegal S. *Nonparametric Statistics for the Behavioral Sciences.* New York, NY: McGraw-Hill International Book Co; 1956.
18. Dix RD, Hurst L, Keane RW. Herpes simplex virus type 1 infection of mouse astrocytes treated with basic fibroblast growth factor. *J Gen Virol.* 1992;73:1845-1848.
19. Gressens P, Martin J. HSV-2 DNA persistence in astrocytes of the trigeminal root entry zone: double labeling by in situ PCR and immunohistochemistry. *J Neuropathol Exp Neurol.* 1994;53:127-135.
20. Thomas EE, Lau AS, Kim SU, Osborne D, Kastrukoff LF. Variation in resistance to herpes simplex virus type 1 of oligodendrocytes derived from inbred strains of mice. *J Gen Virol.* 1991;72:2051-2057.
21. Nicoll JAR, Kinrade E, Love S. PCR-mediated search for herpes simplex virus DNA in sections of brain from patients with multiple sclerosis and other neurological disorders. *J Neurol Sci.*1992;113:144-151.
22. Alexander RC, Cabirac G, Lowenkopf T, et al. Search for evidence of herpes simplex virus, type 1, or varicella-zoster virus infection in postmortem brain tissue from schizophrenic patients. *Acta Psychiatr Scand.* 1992;86:418-420.
23. Jamieson GA, Maitland NJ, Wilcock GK, Craske J, Itzhaki RF. Latent herpes simplex virus type 1 in normal and Alzheimer's disease brains. *J Med Virol.* 1991;33:224-227.

STIC-ILL

From: Gambel, Phillip
Sent: Tuesday, July 23, 2002 4:00 PM
To: STIC-ILL
Subject: refernces of recrod in ussn 09 / 010377 rubin encephalitis

stic

please provide the following references to

phillip gambel
art unit 1644
308-3997

1644 mailbox 9E12

---

1) sanders et al. archives of neurology 53 : 125- 133 (1996)

2) editorial archives of neurology 53 : 123- 124 (1996)

3) soilo-hanninen et al. scand. j. immunol. 43 : 727 - ? (1996)

4) soilo-hanninen et al. j. neuroimmunol. 72 : 95 - 105 (1997)

5) planz et al. j. virol. 69 : 896 - 903 (1995)

thanx

NU>

ADONIS 20-

~~RC346. J68~~

Article title	Therapy with antibody against leukocyte integrin VLA-4(CD49d) is effective and safe in virus-facilitated experimental allergic encephalomyelitis
Article identifier	0165572897000108
Authors	Soilu-Hanninen_M Roytta_M Salmi_A Salonen_R
Journal title	Journal of Neuroimmunology
ISSN	0165-5728
Publisher	Elsevier Netherlands
Year of publication	1997
Volume	72
Issue	1
Supplement	0
Page range	95-105
Number of pages	11
User name	Adonis
Cost centre	Development
PCC	$20.00
Date and time	Wednesday, July 24, 2002 9:48:19 AM

ELSEVIER

Journal of Neuroimmunology 72 (1997) 95–105

Journal of Neuroimmunology

Therapy with antibody against leukocyte integrin VLA-4 (CD49d) is effective and safe in virus-facilitated experimental allergic encephalomyelitis

M. Soilu-Hänninen [a,*], M. Röyttä [b], A. Salmi [a], R. Salonen [a,1]

[a] *Department of Virology, University of Turku, Kiinamyllynkatu 13, FIN-20520 Turku, Finland*
[b] *Department of Pathology, University of Turku, Turku, Finland*

Received 6 May 1996; revised 8 August 1996; accepted 9 August 1996

Abstract

Experimental allerigic encephalomyelitis (EAE) is facilitated in resistant BALB/c mice by intraperitoneal infection with an avirulent Semliki Forest virus (SFV-A7). Viral infection increases the incidence of EAE from 15–30% to 60–90% and speeds up appearance of paralysis from 24 to 14 days. In this paper, we describe treatment of virus-facilitated EAE with monoclonal antibodies (mAbs) against leukocyte and/or endothelial cell adhesion molecules. Therapy with mAb against ICAM-1 (intercellular adhesion molecule-1) had a modest effect, but caused hemorrhagic brain and spinal cord lesions. Therapy with mAb against Mac-1 ($\alpha_M \beta_2$-integrin) was well tolerated but had no effect. Therapy with mAb against VLA-4 ($\alpha_4 \beta_1$-integrin) was safe, diminished both clinical and histopathological signs of EAE, decreased induction of VCAM-1 (vascular cell adhesion molecule-1) on brain vessels and diminished infiltration of VLA-4$^+$ cells into the brain. The amount of viral antigen in the brain was not altered. We conclude that facilitation of leukocyte entry into the brain is a major mechanism for viral facilitation of EAE in the BALB/c mouse, and that facilitation can be inhibited by anti-adhesion therapy. This may have implications for treatment of relapses triggered by viral infections in multiple sclerosis.

Keywords: Experimental allergic encephalomyelitis; Semliki Forest virus infection; Cell adhesion molecules; Multiple sclerosis

1. Introduction

There is no spontaneous animal model that would represent the complexity of the pathogenesis of the human autoimmune-mediated central nervous system (CNS) disease, multiple sclerosis (MS). Experimentally induced allergic encephalomyelitis (EAE) in rodents is considered as a useful model for studying the pathogenesis of MS and hopefully for designing new specific therapies (Raine, 1984; Wekerle et al., 1994). Viral infections can serve as triggers of relapse phases of MS (Sibley et al., 1985; Anderson et al., 1993). To study this specific aspect in the pathogenesis of MS, we have established a model of virus-facilitated EAE in BALB/c mice (Wu et al., 1988; Erälinna et al., 1994). This mouse strain is genetically resistant to EAE induction. Whole body irradiation and subsequent immunization with spinal cord homogenate lead to development of paralysis in 15–30% of mice between 18 and 28 days after injection. Intraperitoneal infection with a non-lethal mutant of a neurotropic Semliki Forest virus (SFV-A7) 7 days after immunization, increases the incidence of EAE to 60–90% and shortens the mean time required for appearance of clinical signs from 24 to 14 days.

Entry of T-cells into the CNS has a pivotal role in the formation of MS lesions (Raine, 1991). Interaction between adhesion receptors on leukocytes and their endothelial ligands is a prerequisite for transendothelial migration. Both members of the immunoglobulin (Ig) superfamily and integrin family of adhesion receptors have been implicated in T-cell recruitment into brain in MS (Sobel et al., 1990; Washington et al., 1994; Svenningsson et al., 1993). Inhibition of lymphocyte migration across endothelial cells

* Corresponding author. Tel.: +358 (21) 633 7461; fax: +358 (21) 251 3303; e-mail: merja.soilu-hanninen@utu.fi
[1] Present address: Glaxo Wellcome, Finland.

PII S0165-5728(96)00158-0

by blocking the function of adhesion receptors by monoclonal antibodies provides an opportunity for therapeutic intervention into CNS autoimmune reactions.

Anti-adhesion receptor therapy has been studied and shown to be effective in many rodent models of EAE. Antibodies against $\alpha 4\beta 1$-integrin (VLA-4) have been shown to inhibit adoptively transferred EAE both in Lewis rats and in PL/J mice (Yednock et al., 1992; Baron et al., 1993). Anti-ICAM-1 therapy has been reported to suppress actively induced EAE in Lewis rats (Archelos et al., 1993). Another group reported that anti-ICAM-1 therapy inhibits both actively induced and adoptively transferred EAE in Lewis rats, but only when combined with LFA-1 antibodies (Kobayashi et al., 1995). Also anti-Mac-1 therapy has been shown to suppress EAE induced by active immunization in Lewis rats (Huitinga et al., 1993). Both LFA-1 and Mac-1 antibodies were recently reported to delay the onset and diminish the severity of adoptively transferred EAE in PL/J mice (Gordon et al., 1995). Antibodies against adhesion receptors will also enter clinical trials involving humans in the near future (Lobb and Hemler, 1994).

We have shown previously, that SFV-A7 infection of mice leads to blood–brain barrier (BBB) damage and increases expression of ICAM-1 on brain vessels (Soilu-Hänninen et al., 1994). This may contribute to the facilitation of EAE by SFV-A7 (Erälinna et al., 1994, 1996). Cells strongly expressing the $\alpha_M \beta_2$-integrin, Mac-1, which is involved in macrophage adherence to endothelium, are the most numerous cell type in the CNS mononuclear cell infiltrates in virus-facilitated BALB/c EAE (Erälinna et al., 1994). Increased expression of VLA-4 on $CD8^+$ and $CD4^+$ splenocytes has been suggested to be a general phenomenom associated with systemic viral infections contributing to the homing properties of T-cells during infection (Andersson et al., 1994). Based on these findings and data accumulated from anti-adhesion receptor therapy experiments in other EAE models, we chose anti-ICAM-1, anti-Mac-1 and anti-VLA-4 mAbs for in vivo treatment experiments of Semliki Forest virus-facilitated BALB/c EAE.

In this paper we present results of clinical, histopathological and immunohistochemical studies of the effect of anti-adhesion receptor therapy on virus-facilitated EAE. Anti-ICAM-1 mAb had a modest clinical effect, but caused hemorrhagic lesions in the CNS. Anti-Mac-1 therapy was well tolerated, but ineffective. Anti-VLA-4 therapy diminished clinical signs of EAE and led to a marked reduction in the CNS inflammatory lesions. The amount of viral antigen in the brain was not altered and therapy did not result in any evident clinical or histopathological adverse events. The results indicate that the major mechanism by which SFV-A7 infection facilitates EAE in the BALB/c mouse is the facilitation of leukocyte entry into the CNS via VLA-4/VCAM-1-pathway. The findings may have relevance for future treatment of relapse phases of MS associated with viral infections.

2. Materials and methods

2.1. Mice

BABL/c mice were raised at the Central Animal Laboratory of the University of Turku from breeder stocks obtained from Harlan Sprague–Dawley, Inc., USA. Female mice at age 6 to 8 weeks were used for EAE experiments.

2.2. Virus

An avirulent mutant of Semliki Forest virus (SFV-A7) was obtained from Dr. H.E. Webb (Neurology Unit, Department of Neurology, Rayne Institute, St. Thomas' Hospital, London, UK), plaque purified three times and amplified in a BALB/c mouse brain cell line (MBA-1) previously established in our laboratory. Virus was titrated in another BALB/c brain cell line (MBA-13) using a standard plaque assay. The virus was stored in 1-ml aliquots at -70°C. Virus was used at 1×10^6 plaque forming units (PFU)/mouse injected intraperitoneally (i.p.) in 100 μl of sterile phosphate-buffered saline (PBS).

2.3. Monoclonal antibodies

Hybridomas producing rat mAbs against murine ICAM-1 (IgG_{2a}, clone YN/1.7.4.), Mac-1/CD11b (IgG_{2b}, clone 5C6), VLA-4 (IgG_{2b}, clone PS/2) and anti-mouse macrophage surface marker, *F4/80* (IgG_{2b}, *isotype* matched control mAb for anti-Mac-1 and anti-VLA-4) were from ATCC (American Type Culture Collection, Rockville, MD). Rat anti-mouse syndecan mAb 281.2 (IgG_{2a}, isotype matched control mAb for anti-ICAM-1) was purchased as purified, concentrated mAb from Turku Biotechnology Center, Turku, Finland. For production of mAbs for in vivo injections, the hybridomas were grown in serum-free and protein-free growth medium (Catalog No. S-2772, Sigma, St. Louis, MO, USA). Protein was precipitated from cell-free supernatants with saturated ammonium sulfate (340 g/l of $(NH4)_2SO_4$ at $+4$°C) and dialyzed against PBS. Purity of the mAbs was verified by sodium dodecyl sulfate-polyacrylamide gel electrophoresis (SDS-PAGE) and all aliquots to be used were essentially free from contaminating proteins. Protein concentrations were determined by Ultrospec K 4053 spectrophotometer (LKB Biokrom, Cambridge, UK) based on optical density values at 280 nm. MAbs were adjusted to a final concentration of 1 mg/ml in PBS and sterilized by filtration (0.2 μm filter from Millipore, Bedford, MA). Total of 0.1 mg (100 μl) of mAb was injected i.p. into mice every other day. For immunohistochemistry, anti-VCAM-1 mAb (CD106) was purchased from Pharmingen (San Diego, USA) and the hybridoma producing anti-LFA-1 (CD11a, clone M17/5.2) mAb was from ATCC. Anti-SFV-A7 antibodies were produced in our laboratory by immunization of rabbits with

purified inactivated SFV-A7. Vectastain anti-rabbit and anti-rat antibody staining kits were purchased from Vector Laboratories (Burlingame, CA, USA).

2.4. Induction of EAE

6–8-week-old female BALB/c mice were whole body irradiated with 3.5 Gy using a linear accelerator (4 MeV photons) at the Department of Radiation Therapy and Oncology, Turku University Hospital, Turku, Finland. Two days after irradiation, 100 μl of suspension containing 3 mg of lyophilized mouse spinal cord homogenate (MSCH) in 50 μl of sterile PBS and 50 μl of complete Freund's adjuvant (CFA), was injected into hind footpads of mice. At days 1 and 3 after injection of neuroantigen, 100 ng of pertussis toxin (Islet-activating protein, List Biological Laboratories, USA) in 100 μl of PBS was injected i.v. via the tail vein. Seven days after administration of neuroantigen, mice were infected i.p. with 1×10^6 PFU of SFV-A7 in 100 μl of sterile PBS except for one group of mice that was not infected (Table 1, Experiment 4). All animal experiments were approved by the ethics committee of the local state authorities.

2.5. Evaluation of clinical symptoms

The severity of disease was evaluated daily using the following scale: 0, no clinical symptoms; 1, fur ruffing; 2, tail atonia, slight hind limb paralysis; 3, paraplegia affecting one or both hind limbs; 4, total paralysis or moribund state; 5, death. Only mice that proceeded to grade 3 or more (developed a clear paralysis) were counted in the incidence figures of EAE.

2.6. Histology and immunohistochemistry

At the peak of the clinical disease, 15 days after immunization, 4 mice in the control mAb group and 4 mice in anti-VLA-4 and anti-ICAM-1 treated groups (Table 1, Experiment 5), were killed and processed for histology. Histological examination was performed also on four anti-ICAM-1-treated but uninfected and unimmunized age- and sex-matched control mice. Mice were deeply anesthetized and perfused through the left cardiac ventricle with phosphate-buffered 4% paraformaldehyde. Brains and spinal cords were removed and immersion fixed for at least 24 h. Tissue samples were then embedded in paraffin.

Table 1
Experimental design and summary of results of anti-adhesion receptor therapy in BALB/c EAE

	mAb treatment period (days after immunization)	Number of paralyzed mice	Day of onset (Mean ± S.E.M.)	Duration of the experiment (days)
Experiment 1 (EAE and SFV-A7)				
PBS	4–14	6/10	14.0 ± 0.6	25
IgG2a control [a]	4–14	5/9 [b]	13.6 ± 0.4	25
anti-ICAM-1	4–14	2/10	14.5 ± 0.5	25
Experiment 2 (EAE and SFV-A7)				
PBS	4–14	6/10	14.0 ± 0.8	25
IgG2b control [c]	4–14	5/10	15.8 ± 0.6	25
anti-VLA-4	4–14	1/10	14.0 ± 0	25
Experiment 3 (EAE and SFV-A7)				
PBS	4–14	6/10	14.0 ± 0.8	25
IgG2b control	4–14	5/10	15.6 ± 0.4	25
anti-Mac-1	4–14	6/10	14.8 ± 0.5	25
Experiment 4 (EAE without SFV-A7)				
IgG2a control	4–18	2/10	26.0 ± 0	30
anti-ICAM-1	4–18	1/10	25.0 ± 0	30
anti-VLA-4	4–18	0/10	—	
Experiment 5 (EAE and SFV-A7, histology) [d]				
IgG2a control	4–14	7/10	14.6 ± 0.4	17
anti-ICAM-1	4–14	4/10	15.0 ± 0.6	17
anti-VLA-4	4–14	1/10	14.0 ± 0	17

[a] Rat anti-mouse syndecan mAb was used as isotype-matched control mAb for anti-ICAM-1. 0.1 mg of mAb was injected i.p. every other day between time points indicated.
[b] Number of mice is 9 instead of 10 because one mouse died immediately after the first injection of mAb.
[c] Rat anti-mouse macrophage marker (F4/80) was used as isotype-matched control mAb for anti-VLA-4 and anti-Mac-1.
[d] Four mice in each group were killed for histology on day 15 and two mice in each group were killed for immunohistochemistry on day 17.

Five-μm thick paraffin sections were stained with hematoxylin and eosin. Sections were scored for inflammatory infiltrates in a blinded fashion by a neuropathologist on the following semiquantitative scale: 0, no inflammatory cells; 1, a few cells; 2, moderate, perivascular cuffings; 3, large inflammatory cell infiltrates, parenchymal necrosis.

Immunoperoxidase staining for detection of SFV-A7 antigens was done on deparaffinized sections with polyclonal rabbit anti-SFV-A7 antibody. Binding of primary antibody was demonstrated by the avidin–biotin complex (ABC) technique with a Vectastain anti-rabbit antibody kit according to the manufacturer's instructions. The color reaction was developed with DAB as chromogen. Sections were counterstained with Mayer's hematoxylin. Amount of viral antigen was assessed in a blinded fashion by a neuropathologist and scored on the following semiquantitative scale: 0, no staining; 1, staining confined to vascular endothelium; 2, staining perivascularly; 3, staining perivascularly and in the CNS parenchyma.

In addition, two mice in each group (Table 1, Experiment 5) were killed and processed for immunohistochemistry at day 17 after immunization. Mice were extensively perfused with PBS under anesthesia. The brains and spinal cords were then removed and rapidly frozen in Tissue Tek (Miles, Naperville, IL) by immersion in liquid nitrogen. The blocks were stored at -70°C until use. Six-μm thick frozen sections were cut on a cryotome, mounted on organosiliconized slides (Maples, 1985), air-dried, fixed in cold acetone for 10 min and preserved at -20°C until use. For immunoperoxidase staining with rat mAbs against murine LFA-1, Mac-1, VLA-4, ICAM-1 and VCAM-1, frozen sections were first incubated for 30 min with nonconjugated goat anti-rat IgG to block cross-reaction with the mAbs injected in vivo. Primary mAbs were then allowed to react overnight at $+4$°C. Binding of primary mAbs was demonstrated with the ABC technique with a Vectastain anti-rat antibody staining kit. Color reaction was developed with DAB. The sections were counterstained with hematoxylin. To demonstrate whether the mAbs injected in vivo had bound to the vascular endothelium/infiltrating cells in the CNS, some of the sections in every treatment group were reacted with secondary mAb only. The number of positively stained cells and their staining intensity was evaluated by an experienced neuropathologist in a blinded fashion and scored on the following semiquantitative scale: 0, no reactive ells; +, a few positive cells/weak staining; ++, moderate; +++, many positive cells on every section/strong staining intensity. Approximately 10 sections/mouse were studied.

2.7. Statistical analysis

An unpaired Student's *t*-test was used to evaluate statistical differences in the developement of EAE between mAb-treated mice and control mice. A P value of less than 0.05 was taken as statistically significant.

3. Results

3.1. Effect of anti-adhesion receptor therapy on the clinical signs of EAE

The experimental design and summary of results of anti-adhesion receptor therapy on the clinical outcome of BALB/c EAE are shown in Table 1.

3.1.1. Anti-ICAM-1

Rat mAb 281.2 (IgG_{2a}) reacting with mouse syndecan was chosen as an isotype-matched control mAb for rat anti-mouse ICAM-1 mAb YN/1.7.4. (IgG_{2a}). YN/1.7.4. reacts with and blocks function of ICAM-1, which is a member of the immunoglobulin superfamily of adhesion receptors and binds to leukocyte integrins LFA-1 and Mac-1 (Springer, 1990). In groups of mice with virus-facilitated EAE treated with PBS or anti-syndecan mAb, 60% of mice developed hind limb paraplegia, whereas only 20% of anti-ICAM-1-treated mice were paralyzed (Table 1). The onset of paralysis did not differ between treated and control mice, but the difference in the incidence of EAE between anti-ICAM-1-treated and control mAb-treated mice was statistically significant ($P < 0.05$).

3.1.2. Anti-Mac-1

Anti-mouse macrophage marker, mAb F4/80, was chosen as a control mAb for anti-VLA-4 and anti-Mac-1 mAbs, because it is isotype-matched (rat IgG_{2b}) and reacts specifically with mouse macrophages. It precipitates a 160,000 dalton glycoprotein, the function of which is unknown. Clone 5C6 reacts with the $\alpha_M \beta_2$-integrin, also known as type 3 complement receptor CR3 (CD11b/Mac-1) and inhibits myelomonocytic cell adhesion in vitro and inflammatory cell recruitment in vivo. However, it did not have any effect on the incidence of virus-facilitated EAE, which was 60% in the 5C6-treated and PBS-treated groups of mice and 50% in the F4/80-treated group of mice (Table 1). Compared with PBS, control mAb F4/80 slightly delayed the onset of EAE and decreased the incidence of EAE from 60% to 50%. This was, however, statistically not significant. Saturation of the mice with 5C6 mAb was demonstrated by flow cytometry. Serum of mice injected with 100 μg or 200 μg of 5C6 in vivo stained a similar 8% population of Mac-1$^+$ cells of all spleen mononuclear cells as a dose of 10 μg/ml of 5C6 mAb used for staining of the cells in parallel in vitro. An in vivo dose of 500 μg/mouse was already too high, since it decreased the proportion of positive cells to 6%, indicating a prozone effect with this dose. Therefore, the inefficacy of anti-Mac-1 treatment in virus-facilitated EAE was not due to insufficient antibody administration.

3.1.3. Anti-VLA-4

$\alpha 4 \beta 1$-integrin, also known as very late activation antigen (VLA-4), is expressed on most leukocytes and medi-

ates adhesion to VCAM-1 and fibronectin (Springer, 1994). Treatment with anti-VLA-4 mAb reduced the incidence of EAE to 10% in two separate experiments. Compared with groups of mice that received either PBS (incidence 60%) or isotype-matched control mAb F4/80 (incidence 50%), the differences were significant difference ($P < 0.05$).

3.1.4. EAE without viral facilitation

Because the IgG_{2b} control mAb F4/80 had an attenuating tendency in the virus-facilitated model of EAE, anti-syndecan mAb (IgG_{2a}) was used as a control mAb both for anti-ICAM-1 (IgG_{2a}) and anti-VLA-4 (IgG_{2b}) mAbs in an in vivo treatment experiment of BALB/c EAE without viral facilitation. In anti-syndecan mAb-treated group, 2 out of 10 mice developed paralysis on day 26, and in anti-ICAM-1-treated group, 1 out of 10 mice on day 25, whereas all anti-VLA-4-treated mice remained clinically healthy. The differences were not significant. Anti-Mac-1 therapy was not studied in EAE without viral facilitation.

3.2. Histopathological signs of EAE and detection of virus antigen in anti-ICAM-1-treated, anti-VLA-4-tretated and control mice

Histopathological analysis was performed in anti-ICAM-1-treated and anti-VLA-4-treated mice to study whether treatment reduced inflammatory changes in the CNS and whether it had an effect on the amount of virus antigen expression in the brain. As a control, mice treated with control mAb were analyzed. Histology was not performed in anti-Mac-1 treated mice, because this mAb had no therapeutic effect in the clinical experiment.

3.2.1. Control

Mice in the control mAb (anti-syndecan)-treated group had moderate mononuclear cell infiltrations in the white matter of the spinal cord, brain stem, cerebellum and thalamus with perivascular cuffing (Fig. 1A and B). In 1 of 4 mice there were two small hemorrhages on 1 of 10 sections studied. There were no macroscopically detectable hemorrhagic lesions. The clinical score of all four histopathologically analyzed control mice was 3 (hind limb paraplegia).

3.2.2. Anti-ICAM-1

In mice treated with anti-ICAM-1 mAbs, the CNS inflammatory changes were moderate in 1 of 4 mice and mild in 3 of 4 mice. The mean clinical score was 1.4. A striking feature was the presence of numerous small petechial hemorrhages throughout the CNS in every mouse. The lesions were macroscopically visible when inspecting the brain and spinal cord tissue. In hematoxylin-eosin-stained sections, endothelial damage and leakage of erythrocytes into the CNS parenchyma were seen (Fig. 1C and D). There were no macroscopically or microscopically detectable hemorrhages in anti-ICAM-1-treated uninfected, unimmunized age- and sex-matched control mice (data not shown).

3.2.3. Anti-VLA-4

Anti-VLA-4 treatment did not completely block the inflammatory response in the CNS of the treated mice, but the inflammatory changes were fewer and milder than in the control mAb-treated mice (Fig. 1E and F) and they were mostly confined to the meninges. In 2 out of 4 mice only minimal meningeal lesions in the spinal cord were detected and the brains were totally devoid of inflammatory cells. There were no hemorrhagic lesions in the CNS.

3.2.4. Virus antigen

In immunostaining for virus antigen, perivascular foci of infected neurons were detected in the spinal cord, cerebellum and cerebral hemispheres in all treated and control mice. In 3 out of 4 mice in all groups there was also staining in the CNS parenchyma (Fig. 1G and H). The amount of viral antigen did not differ significantly between the treatment groups.

Summary of histological findings in anti-ICAM-1- and anti-VLA-4-treated mice and control mice are presented in Table 2.

Table 2
Inflammatory changes and amount of viral antigen in the CNS of mAb-treated mice with EAE and SFV-A7 infection (day 15)

Number of mice	Treatment	Clinical score	Histological score [a]		Amount of viral antigen [b]		Hemorrhagic CNS lesions [c]
			spinal cord	brain	spinal cord	brain	
4	IgG2a control mAb	3.0 ± 0	1.8 ± 0.2	2.0 ± 0.3	2.8 ± 0.3	2.8 ± 0.3	1/4
4	anti-ICAM-1 mAb	1.4 ± 0.4	1.0 ± 0	1.4 ± 0.2	2.8 ± 0.3	2.5 ± 0.3	4/4
4	anti-VLA-4 mAb	1.0 ± 0	0.8 ± 0.3	0.6 ± 0.2	2.5 ± 0.3	2.5 ± 0.3	0/4

[a] Inflammatory cells were identified on hematoxylin-eosin-stained paraffin sections and scored on the following semiquatitative scale: 0, no inflammatory cells; 1, a few cells; 2, moderate, perivascular cuffings; 3, large infiltrates and parenchymal necrotic changes. Values are mean ± S.E.M of histological scores of four mice.

[b] Amount of viral antigen was quantitated on the following semiquantitative scale: 1, staining confined to vascular endothelium; 2, staining perivascularly; 3, staining perivascularly and in the CNS parenchyma. Values represent mean ± S.E.M. of four mice.

[c] Number of mice showing hemorrhagic CNS lesions on hematoxylin-eosin-stained sections of the four mice mice studied is shown.

Table 3
Effect of anti-adhesion receptor therapy on the expression of adhesion molecules and vascular ligands in the CNS of mice with virus-facilitated EAE [a]

Treatment	Clinical score	ICAM-1 CD54	VCAM-1 CD106	LFA-1 CD11a	Mac-1 CD11b	VLA-4 CD49d
Control mAb [b]	3	+ +	+ + +	+ +	+ + +	+ +
Control mAb	3	+ +	+ + +	+ +	+ + +	+
Anti-ICAM-1 mAb	2	+ +	+ + +	+ +	+ + +	+
Anti-ICAM-1 mAb	2	+ +	+ + +	+ +	+ + +	+
Anti-VLA-4 mAb	1	+	+	+	+ + +	0
Anti-VLA-4 mAb	1	+ +	+ +	+ +	+ + +	+

[a] Two mice in each treatment group were killed at the height of the clinical symptoms (EAE day 17). Immunohistochemical staining of frozen sections of spinal cord, cerebellum and cerebral hemispheres was done as described in Section 2.6. The number of reactive cells and their staining intensity was evaluated by a neuropathologist in a blinded fashion using the following semiquantitative scale: 0, no reactive cells; +, a few positive cells, weak staining; + + reactive cells on every section, moderate staining intensity; + + +, many positive cells on every section/strong staining intensity. Circa 10 sections/mouse were studied.
[b] Anti-syndecan mAb (281.2) was used as a control.

3.3. Immunohistochemical findings in anti-ICAM-1-treated, anti-VLA-4-treated and control mice

Immunohistochemical analysis was done to demonstrate saturation of mice with the mAbs injected in vivo and to evaluate the expression of immunologically relevant adhesion molecule/ligand pairs ICAM-1/LFA-1 or Mac-1 and VCAM/VLA-4 in treated and control mice. Anti-Mac-1-treated mice were not analyzed due to lack of therapeutic effect with this mAb.

In EAE mice treated with anti-ICAM-1 mAb, staining with secondary antibody alone showed that the mAb against ICAM-1 administered in vivo had bound to the CNS vascular endothelium (Fig. 2A and B). The mice received the last injection of mAb 3 days before being killed for immunohistochemical analysis, indicating that the dosage regimen used (0.1 mg every other day between days 4 and 14) was saturating. In mice treated with anti-syndecan mAb (Fig. 2C) or anti-VLA-4 mAb, no reactivity could be seen with secondary mAb alone, because CNS endothelial cells do not express these antigens and the mAbs apparently do not cross the BBB.

Compared with the low basal level of ICAM-1 expression in normal BALB/c mouse brain, all the treated and control mice had induction of ICAM-1 on CNS vessels and infiltrating mononuclear cells. Expression of ICAM-1 was more diffuse than the virus antigen staining. Level of ICAM-1 expression was estimated to be moderate in the control mAb-treated and in the ICAM-1 mAb-treated mice. In the VLA-4 group, ICAM-1 staining was weak in one and moderate in the other of the two mice processed for immunohistochemistry.

The ligands for ICAM-1, i.e. lymphocyte function associated antigen-1, LFA-1 (CD11a) and Mac-1 (CD11b), were expressed in the CNS of all the treated and control mice. Mac-1^+ cells were more numerous than LFA-1^+ cell with many positive cells and strong staining intensity in all the mice. A moderate number of LFA-1^+ cells were detected both in anti-ICAM-1-treated and control mice and few to moderate in anti-VLA-4-treated mice. LFA-1^+ cells were mostly confined to perivascular cuffings, whereas Mac-1^+ cells were diffusely distributed in the white matter of the spinal cord, cerebellum, brain stem and cerebral hemispheres.

Strikingly strong expression of VCAM-1 was detected in the control mAb-treated and anti-ICAM-1 mAb-treated mice. VCAM-1 was expressed in the vascular endothelium diffusely throughout the CNS showing clear predilection to the white matter. In the most strongly positive areas in the cerebellar, brain stem and spinal cord white matter, all vessels were intensely immunoreactive with VCAM-1 (Fig. 2D). Also the luminal surface of the ependymal cells lining the cerebral ventricles strongly expressed VCAM-1. In contrast, mice treated with anti-VLA-4 mAb had only weak to moderate expression of VCAM-1 in the CNS white matter (Fig. 2E).

Fig. 1. Histological analysis of CNS inflammation in BALB/c mice with virus-facilitated EAE treated with control mAb (anti-syndecan), mAb against ICAM-1 or mAb against VLA-4. Mice were killed at the height of the clinical symptoms (on day 15) and the paraffin-embedded CNS sections were stained with hematoxylin and eosin. (A and B) A typical perivascular cuffing (arrows in A and the area marked with open arrow in B) in cerebral hemisphere in a clinically paralyzed mouse treated with control mAb. (C and D) Hemorrhagic cerebral lesions (arrows) in the region of nucleus caudatus in a mouse treated with anti-ICAM-1 mAb. Area indicated with open arrow is shown at higher magnification in (D), where numerous extravascular red blood cells are noted (arrows). (E and F) Maximal inflammatory infiltrate in the hippocampus of a mouse treated with anti-VLA-4 mAb. Note that in (E), the obvious perivascular inflammatory cells are located only around one vessel (shown by higher magnification in (F)), while the other two vessels in (E) appear to be normal. (G and H) Detection of Semliki Forest virus antigens by immunoperoxidase staining with rabbit polyclonal anti-SFV-A7 antiserum in the cerebellum of an EAE mouse treated with control mAb (EAE day 15, 7 days after i.p. infection with SFV-A7). White matter is indicated with an asterisk and molecular cell layer with a star. Purkinje cells cell bodies (curved arrow) were strongly positive, as well as the dendrites. Bar in (A) represents 0.6 mm in (A), 30 μm in (B) and (F), 0.7 mm in (C), 35 μm in (D), 70 μm in (E), 0.8 mm in (G) and 150 μm in (H).

In control mice and mice treated with anti-ICAM-1 mAb, VLA-4-expression was detected on a few inflammatory cells scattered in the CNS parenchyma or on small clusters of 5–15 positive cells in the perivascular cuffings (Fig. 2F). VLA-4$^+$ cells could not be detected in one of the two studied anti-VLA-4-treated mice, and only few

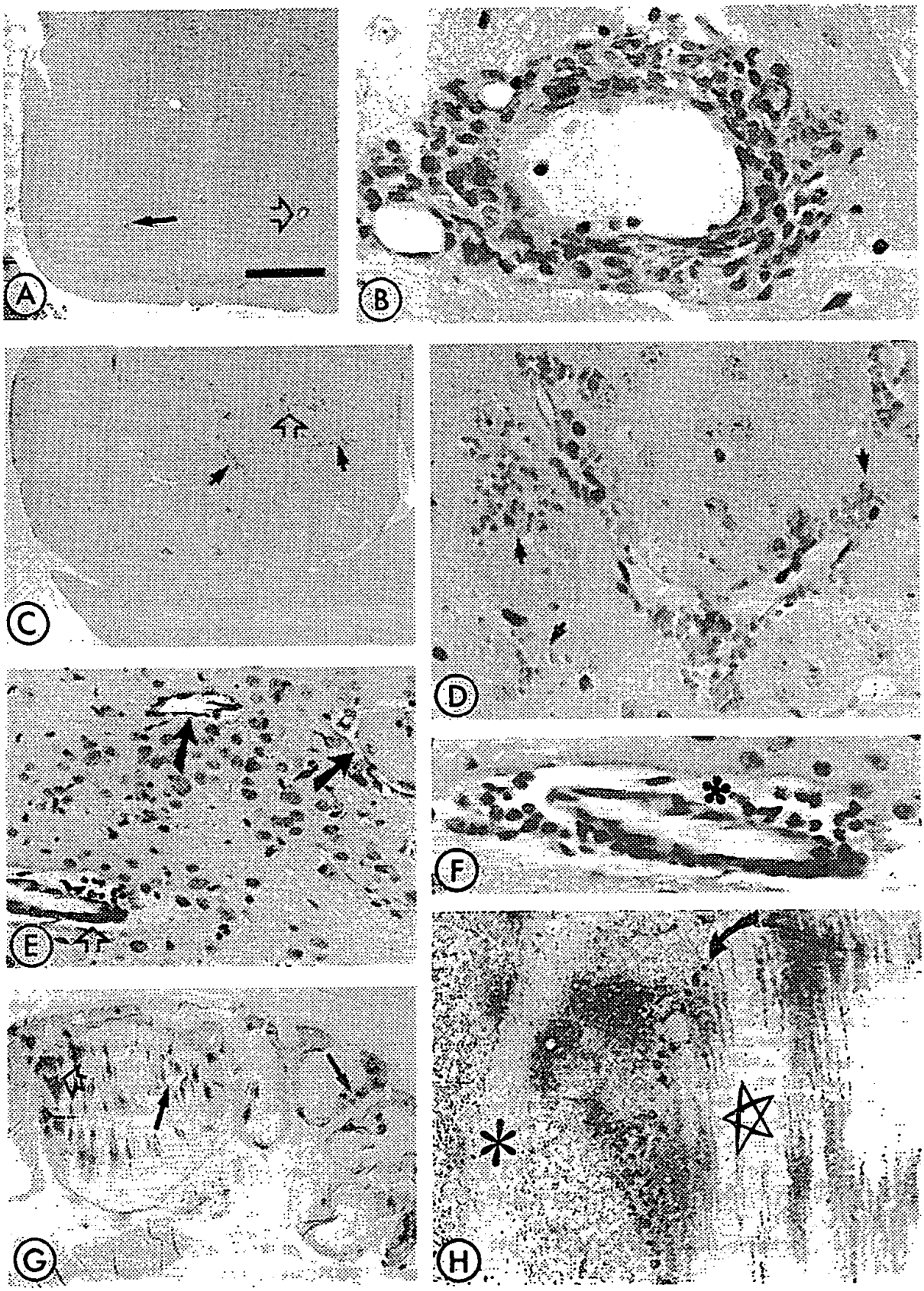

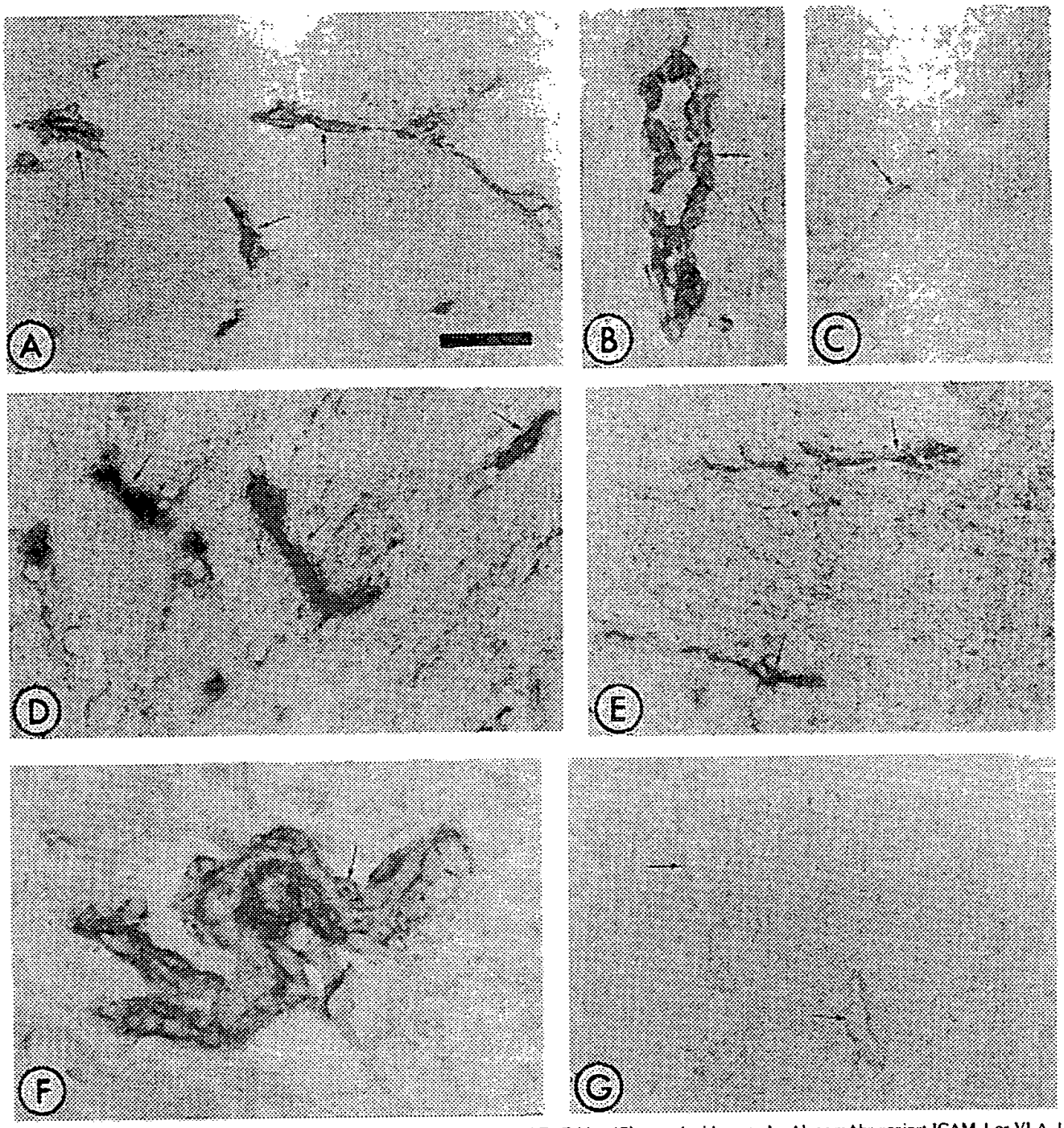

Fig. 2. Immunohistochemical analysis of BALB/c mice with virus-facilitated EAE (day 17) treated with control mAb or mAbs against ICAM-1 or VLA-4. Immunoperoxidase staining on frozen CNS sections was done using the ABC-technique. (A and B) Brain stem section of a mouse treated with anti-ICAM-1 mAbs stained with secondary antibody only to demonstrate binding of the in vivo injected mAb to brain vessels. (C) No staining in a brain stem section of an anti-syndecan mAb-treated mouse reacted with secondary antibody only since syndecan is not expressed on brain endothelial cells. (D) Strongly induced expression of VCAM-1 on cerebral vessels in a mouse treated with control mAb. (E) Weak staining with with anti-VCAM-1 mAb on spinal cord vessels in an anti-VLA-4-treated mouse. (F) VLA-4$^+$ cells in cerebral white matter in a mouse treated with control mAb. (G) VLA-4 + cells were absent or few in the cerebral white matter of anti-VLA-4-treated mice. Vessels are marked by arrows. Bar in (A) represents 30 μm in (A), (B), (D) and (G), 35 μm in (C) and (E) and 25 μm in (F).

weakly stained cells were identified in the other VLA-4-treated mouse (Fig. 2G).

Summary of the immunohistochemical findings are presented in Table 3.

4. Discussion

We have shown previously that infection of mice with Semliki Forest virus leads to BBB damage and increased

expression of ICAM-1 on brain endothelial cells. This and our work in EAE have led to a hypothesis that facilitated entry of leukocytes into the CNS is a major mechanism contributing to facilitation of EAE in the BALB/c mouse by SFV-A7 infection (Soilu-Hänninen et al., 1994; Erälinna et al., 1994, 1996). The aim of the present study was to investigate further whether the viral facilitation of EAE is due to a direct effect of virus in the CNS or caused by the accompanying immune response. The other goal was to determine whether immunotherapy with antibodies against leukocyte and endothelial cell adhesion molecules would be safe and effective in suppressing virus-facilitated EAE.

Upregulation of ICAM-1 expression on brain vasculature has been demonstrated to closely correlate with relapsing autoimmune demyelination in the CNS (Cannella et al., 1990). However, the functional role of ICAM-1-dependent pathway in CNS inflammatory processes is still unclear. A study examining the role of ICAM-1 in the pathogenesis of EAE and TNFα-induced CNS inflammation suggested that the rat homolog of ICAM-1 is not critically involved in the effector phase of CNS inlammation, but may be important in the initial generation of effector cells (Willenborg et al., 1993). This was supported by another study demonstrating an effect with anti-ICAM-1 treatment in actively induced, but not in passive transfer EAE in rats (Archelos et al., 1993). The authors of the latter paper reported spleen necrosis as a surprising side effect of anti-ICAM-1 treatment.

In our virus-facilitated model of actively induced EAE, immunotherapy with a rat anti-mouse ICAM-1 mAb (IgG_{2a} subclass) was partially effective against the clinical and histopathological signs of EAE. A striking finding in the anti-ICAM-1-treated EAE mice was presence of hemorrhagic CNS lesions not observed in mice treated with isotype-matched control mAb or three other mAbs (IgG_{2b} subclass) used in the study. The in vivo injected anti-ICAM-1 mAb was demonstrated to bind to ICAM-1 induced on the CNS endothelium. The formed immunocomplexes may have activated the classical pathway of complement leading to complement-mediated endothelial cell lysis. This is supported by lack of hemorrhages in anti-ICAM-1 treated uninfected and unimmunized control mice, which have undetectable or very low levels of ICAM-1 on brain vessels. The same anti-ICAM-1 mAb (clone YN/1.7.4) has previously been shown to markedly delay the onset of adoptively transferred EAE in PL/J mice (Baron et al., 1993). No side effects were reported in that study, but histopathological examination of the CNS was apparently not done. Our findings suggest that unexpected side effects may occur when anti-adhesion therapy affecting the immune system is applied, which indicates careful safety monitoring and may even preclude application to human use.

The same antibody against the type 3 complement receptor, CR3 (Mac-1/CD11b, clone 5C6), that we used in this study, has previously been shown to block myelomonocytic cell recruitment and extravasation to sites of inflammation (Rosen et al., 1989), inhibit autoimmune diabetes in NOD mice (Hutchings et al., 1990) and delay the onset and diminish the severity of adoptively transferred EAE in PL/J mice (Gordon et al., 1995). However, it did not have any effect on the virus-facilitated model of EAE, although cells expressing the Mac-1 receptor are the most numerous cell type in the CNS inflammatory cell infiltrates in this EAE model. This may indicate, that these cells are not macrophages derived from the circulating monocyte population, but represent the activated form of resident tissue macrophages/microglial cells. Alternatively, monocytes could utilize the LFA-1/ICAM-1 or VLA-4/VCAM-1 pathways for endothelial adhesion and VLA-4 binding to VCAM-1 or homophilic interaction of platelet/endothelial cell adhesion molecule (PECAM, CD31) for transendothelial migration into the CNS, when the Mac-1 receptors are blocked (Luscinscas et al., 1994; Meerschaert and Furie, 1995; Muller, 1995).

Strong evidence from adoptive transfer models of EAE support a critical role for the VLA-4/VCAM-1 pathway in leukocyte migration into inflamed CNS (Yednock et al., 1992; Baron et al., 1993). In this paper we show that anti-VLA-4 therapy is effective, also in our virus-facilitated model of EAE. The amount of virus antigen in the brain was not altered by the treatment. The results confirm our earlier hypothesis that facilitation of leukocyte entry into the CNS is a major mechanism for facilitation of EAE in the BALB/c mouse by SFV-A7 infection.

Upregulation of VLA-4 on spleen T-cells during lymphocytic choriomeningitis virus infection has been shown to be important for effector T-cell influx into the cerebrospinal fluid (Andersson et al., 1994). The same group showed later, that the virus-activated T-cells entering the brain are crucially important in regulating the expression of ICAM-1 and VCAM-1 on brain vessels (Marker et al., 1995). One putative mechanism of action of anti-VLA-4 therapy in our model is inhibition of the entry of the virus specific T-cells into the CNS and prevention of priming of the CNS endothelium by them. This is supported by the immunohistochemical data that showed decreased expression of ICAM-1 and VCAM-1 in the CNS of the anti-VLA-4-treated mice compared with control mAb-treated mice. Inhibition of VLA-4-positive virus-specific cytotoxic T-cells from entering into the brain could also prevent the $CD8^+$ T-cell-mediated destruction of virus-infected oligodendrocytes and thus prevent lesions of demyelination caused by SFV-A7, like in vivo depletion of $CD8^+$ T-cells does (Subak-Sharpe et al., 1993).

A high level of VLA-4 expression is also a feature of MBP-specific encephalitogenic T-cells and correlates with their capacity to induce EAE (Baron et al., 1993). We have earlier confirmed that sensitization to CNS antigens is a prerequisite for development of EAE in BALB/c mice by showing that a protocol combining irradiation and immunization with Freund's adjuvant alone followed by pertus-

sis toxin injections does not lead to disease (Erälinna et al., 1994). Therefore, the efficacy of anti-VLA-4 therapy in virus-facilitated EAE could also be explained by blockade of the entry of the encephalitogenic, CNS-antigen specific T-cells into the CNS in addition to inhibition of the migration of the virus-specific T-cells into the brain.

The findings of this work may have implications for treatment/prevention of MS relapses triggered by viral infections. The mechanisms behind exacerbations of MS are not known. However, activation of autoreactive T-cells in the periphery is probably involved, since only activated T-cells can cross the BBB to initiate a local immune response in the CNS (Wekerle et al., 1986). Viral mimicry peptides can activate human T-cell clones specific for myelin basic protein (Wucherpfennig and Strominger, 1995), which can lead to entry of these cells into the CNS. Vascular endothelium of the CNS is then primed by these activated cells and further influx of inflammatory cells into the CNS compartment follows. Since all potent therapies intervening with the function of the immune system may have harmful side effects, a therapy that could be initiated on demand and discontinued after a short period would be more favourable than continuous therapy. It was recently shown, that circulating ICAM-1 is an early and sensitive marker for virus-induced T-cell activation (Christensen et al., 1995). Patients at risk of developing a relapse in association with a viral infection could be identified by this method. Treatment with effective therapy could then be initiated and continued past the period at risk. This therapy could be e.g. anti-VLA-4 mAb to block the entry of activated T-cells into the CNS.

Acknowledgements

This work was supported by grants from the Turku University Foundation and Sigrid Juselius Foundation. We thank Mrs. Merja Virtanen, Mrs. Marja Aaltonen and Ms. Johanna Ravaska for skillful technical assistance. Ph. Lic. Jarmo Kulmala is acknowledged for arranging the irradiations of the mice.

References

Anderson, O., Lygner, T., Bergström, T., Anderson, M. and Vahlne, A. (1993) Viral infections trigger multiple sclerosis relapses: a prospective seroepidemiological study. J. Neurol. 240, 417–422.

Andersson, E.C., Christensen, J.P., Marker, O. and Thomsen, A.R. (1994) Changes in cell adhesion molecule expression on T-cells associated with systemic virus infection. J. Immunol. 152, 1237–45.

Archelos, J., Jung, S., Mäurer, M., Schmied, M., Lassmann, H., Tamatani, T., Miyasaka, M., Toyka, K. and Hartung, H.P. (1993) Inhibition of experimental allergic encephalomyelitis by an antibody to the intercellular adhesion molecule ICAM-1. Ann. Neurol. 34, 145–154.

Baron, J.L., Madri, J.A., Ruddle, N.H., Hashim, G. and Janeway, C.A. (1993) Surface expression of alpha4 integrin by CD4 T-cells is required for their entry into brain parenchyma. J. Exp. Med. 177, 57–68.

Cannella, B., Cross, A. and Raine, C. (1990) Upregulation and coexpression of adhesion molecules correlate with relapsing autoimmune demyelination in the central nervous system. J. Exp. Med. 172, 1521–1524.

Christensen, J.P., Johansen, J., Marker, O. and Thomsen, A.R. (1995) Circulating intercellular adhesion molecule-1 (ICAM-1) as an early and sensitive marker for virus-induced T-cell activation. Clin. Exp. Immunol. 102, 268–273.

Erälinna, J.P., Soilu-Hänninen, M., Röyttä, M., Hukkanen, V., Salmi, A.A. and Salonen, R. (1996) Blood–brain barrier breakdown and increased intercellular adhesion molecule (ICAM-1/CD54) expression after Semliki Forest (A7) virus infection facilitate the development of experimental allergic encephalomyelitis. J. Neuroimmunol., in press.

Erälinna, J.P., Soilu-Hänninen, M., Röyttä, M., Ilonen, J., Mäkelä, M., Salmi, A. and Salonen, R. (1994) Facilitation of experimental allergic encephalomyelitis by irradiation and virus infection: role of inflammatory cells. J. Neuroimmunol. 55, 81–90.

Gordon, E.J., Myers, K.J., Dougherty, J.P., Rosen, H. and Ron, Y. (1995) Both anti-CD11a (LFA-1) and CD11b (Mac-1) therapy delay the onset and diminish the severity of experimental autoimmune encephalomyelitis. J. Neuroimmunol. 62, 153–160.

Huitinga, I., Damoiseaux, J.G.M.C., Döpp, E.A. and Dijkstra, C.D. (1993) Treatment with anti-CR3 antibodies ED7 and ED8 suppress experimental allergic encephalomyelitis in Lewis rats. Eur. J. Immunol. 23, 709–715.

Hutchings, P.R., Rosen, H., O'Reilly, L., Simpson, E., Gordon, S. and Cooke, A. (1990) Transfer of diabetes in mice prevented by blockade of adhesion promoting receptor on macrophages. Nature 348, 639–642.

Kobayashi, Y., Kawai, K., Honda, H., Tomida, S., Niimi, N., Tamatani, T., Miyasaka, M. and Yoshikai, Y. (1995) Antibodies against leukocyte function-associated antigen-1 and against intercellular adhesion molecule-1 together suppress the progression of experimental allergic encephalomyelitis. Cell. Immunol. 164, 295–305.

Lobb, R.R. and Hemler, M.E. (1994) The pathophysiologic role of $\alpha 4$ integrins in vivo. J. Clin. Invest. 94, 1722–1728.

Luscinscas, F.W., Kansas, G.S., Ding, H., Pizcueta, P., Schleiffenbaum, T.F., Tedder, T.F. and Gimbrone, M.A.J. (1994) Monocyte rolling, arrest and spreading on IL-4-activated vascular endothelium under flow is mediated by sequential action of L-selectin, $\beta 1$-integrins, and $\beta 2$-integrins. J. Cell Biol. 125, 1417–1427.

Maples, J.A. (1985) A method for the noncovalent attachement of cells to glass slides for use in immunohistochemical assays. Am. J. Clin. Pat. 83, 356–363.

Marker, O., Scheynius, A., Christensen J.P. and Thomsen, A.R. (1995) Virus-activated T-cells regulate expression of adhesion molecules on endothelial cells in sites of infection. J. Neuroimmunol. 62, 35–42.

Meerschaert, J. and Furie, M.B. (1995) The adhesion molecules used by monocytes for migration across endothelium include CD11a/CD18, CD11b/CD18, and VLA-4 on monocytes and ICAM-1, VCAM-1, and other ligands on endothelium. J. Immunol. 154, 4099–4112.

Muller, W.A. (1995). The role of PECAM-1 (CD31) in leukocyte migration: studies in vitro and in vivo. J. Leukoc. Biol. 57, 523–528.

Raine, C. (1984) Biology of disease. Analysis of autoimmune demyelination: its impact upon multiple sclerosis. Lab. Invest. 50, 608–635.

Raine, C.S. (1991) Multiple sclerosis: a pivotal role for the T-cell in lesion development. Neuropathol. Appl. Neurobiol. 17, 265–274.

Rosen, H., Milon, G. and Gordon, S. (1989) Antibody to the murine type 3 complement receptor inhibits T-lymphocyte-dependent recruitment of myelomonocytis cells in vivo. J. Exp. Med. 169, 535–548.

Sibley, W.A., Bamford, C.R. and Clark, K. (1985) Clinical viral infections and multiple sclerosis. Lancet ii, 1313–1315.

Sobel, R., Mitchell, M. and Fondren, G. (1990) Intercellular adheston

molecule-1 (ICAM-1) in cellular immune reactions in the human central nervous system. Am. J. Pat. 136, 1309–1316.

Soilu-Hänninen, M., Erälinna, J.P., Hukkanen, V., Röyttä, M., Salmi A.A. and Salonen, R. (1994) Semliki Forest virus infects mouse brain endothelial cells and causes blood–brain barrier damage. J. Virol. 68, 6291–6298.

Springer, T.A. (1990). Adhesion receptors of the immune system. Nature 346, 425–433.

Springer, T.A. (1994). Traffic signals for lymphocyte recirculation and leukocyte emigration: the multistep paradigm. Cell 76, 301–314.

Subak-Sharpe, I., Dyson, H. and Fazakerley, J. (1993) In vivo depletion of CD8+ T-cells prevents lesions of demyelination in Semliki Forest virus infection. J. Virol. 67, 7629–7633.

Svenningsson, A., Hansson G., Andersen O., Andersson R., Patarroyo M. and Stemme, S. (1993) Adhesion molecule expression on cerebrospinal fluid T lymphocytes: Evidence for common recruitment mechanisms in multiple sclerosis, aseptic meningitis and normal controls. Ann. Neurol. 34, 155–161.

Washington, R., Burton, J., Todd, R.F., Newman, W., Dragovic, L. and Dore-Duffy, P. (1994) Expression of immunologically relevant endothelial cell activation antigens on isolated central nervous system microvessels from patients with multiple sclerosis. Ann. Neurol. 35, 89–97.

Wekerle, H., Kojima, K., Lannes-Vieira, J., Lassmann, H. and Linington, C. (1994) Animal Models. Ann. Neurol. 36, S47–S53.

Wekerle, H., Linington, C., Lassman, H. and Meyermann, R. (1986) Cellular immune reactivity within the CNS. Trends in Neurosci. Res. 9, 271–277

Willenborg, D.O., Simmons, R.D., Tamatani, T. and Miyasaka, M. (1993) ICAM-1-dependent pathway is not critically involved in the inflammatory process of autoimmune encephalomyelitis or in cytokine-induced inflammation of the central nervous system. J. Neuroimmunol. 45, 147–154.

Wu, L.-X., Mäkelä, M.J., Röyttä, M. and Salmi, A. (1988) Effect of viral infection on experimental allergic encephalomyelitis in mice. J. Neuroimmunol. 18, 139–153.

Wucherpfennig, K.W. and Strominger, J.L. (1995). Molecular mimicry in T-cell-mediated autoimmunity: viral peptides activate human T-cell clones specific for myelin basic protein. Cell 80, 695–705.

Yednock, T., Cannon, C., Fritz, L.C., Sanchez-Madrid, F., Steinmann, L. and Karin, N. (1992) Prevention of experimental autoimmune encephalomyelitis by antibodies against $\alpha 4\beta 1$ integrin. Nature (Lond.) 356, 63–66.

STIC-ILL

From: Gambel, Phillip
Sent: Tuesday, July 23, 2002 4:00 PM
To: STIC-ILL
Subject: refernces of recrod in ussn 09 / 010377 rubin encephalitis

MIC
RC321.A67

stic

please provide the following references to

phillip gambel
art unit 1644
308-3997

1644 mailbox 9E12

---

1) sanders et al. archives of neurology 53 : 125- 133 (1996)

2) editorial archives of neurology 53 : 123- 124 (1996)

3) soilo-hanninen et al. scand. j. immunol. 43 : 727 - ? (1996)

4) soilo-hanninen et al. j. neuroimmunol. 72 : 95 - 105 (1997)

5) planz et al. j. virol. 69 : 896 - 903 (1995)

thanx

EDITORIAL

Herpesviruses in Multiple Sclerosis

In this issue of the ARCHIVES, Sanders et al[1] report on the presence of herpes simplex virus (HSV) 1 and 2 in 46% of postmortem brain tissue samples from patients with multiple sclerosis and in 28% of samples from control cases. In the August 1995 issue of the *Proceedings of the National Academy of Science,* Challoner et al[2] report on the presence of human herpesvirus 6 (HHV-6) in brain samples from patients with MS. These two articles represent the latest among many reports of viruses detected in MS brain by culture, hybridization techniques, or immunocytochemical methods. Are these simply observations on the normal viral flora found in the brain, perhaps enhanced in the MS brains by the use of immunosuppressive agents and steroids? While the observations on HHV-6 have been met with underwhelming enthusiasm, there are a number of reasons why such observations deserve careful examination.

See also page 125

Human herpesvirus 6 is transmitted by a respiratory route and is the agent that causes exanthem subitum, or roseola infantum. Herpes simplex virus 1 is a common infection that usually causes pharyngitis initially and then produces recurrent herpes febrilis, commonly referred to as *fever blisters* or *cold sores.* Herpes simplex virus 2 is a common sexually transmitted genital infection with virus latency in the sacral ganglia. There are a variety of reasons why the herpesviruses, and particularly HHV-6, are worthy of further investigation to clarify their relationship to MS:

1. The method of detecting HHV-6 using polymerase chain reaction and representational difference analysis techniques was not previously available to pick up foreign, ie, non–human DNA, in MS brains. Presumably, HHV-6 was present in much larger amounts than HSV-1 or HSV-2, since it was the one most readily detected.

2. Although Challoner et al[2] found virus in 78% of MS brains and in 74% of control brains, they demonstrated that the virus was present not only in MS plaques but also in neurons and especially in oligodendrocytes in plaques. The virus was found much less frequently in normal-appearing white matter. Staining of oligodendrocytes was detected in 12 of 15 MS cases and in none of 45 control cases, even though virus was frequently detected in the brains of control cases. Thus, the virus is present not only in the plaques but in the relevant cells.

3. Most, if not all, herpesviruses are latent in nervous tissue and, when latent, cannot be structurally identified, so they would not be likely to be found on electron microscopy.

4. Herpesvirus activation and MS exacerbations are both known to be precipitated by other viral infections.

5. A number of herpesviruses are known to cause demyelination.

6. Herpesviruses are transported within axons and are spread, in part, by axonal transport. This could easily account for the patchy involvement of the nervous system.

7. Finally, and perhaps a bit fancifully, many childhood infections, including measles, chicken pox, and HSV-1, cause an infrequent chronic or recurrent viral infection that affects the central nervous system as a sequel to the primary illness. Since HHV-6 causes roseola, this would be analogous to other chronic sequelae of childhood exanthems, such as subacute sclerosing panencephalitis and progressive rubella panencephalitis, shingles, and recurrent cutaneous herpes, which is accompanied by a ganglionitis.

The application of these new techniques to the discovery of obscure latent viruses that may periodically reactivate will undoubtedly lead to an improved understanding of the interaction of viruses with their hosts and their role in various disease processes. The work of Sanders et al[1] and of Challoner et al[2] does not establish HHV-6 or herpesviruses as the cause of MS. Koch's postulates have not been fulfilled, but given the species specificity of viruses, as with a number of other diseases, it may never be possible to fulfill them. Nevertheless, the observations are important. Activation of the virus in the central nervous system, by causing expression of type II histocompatibility antigens and disruption of the blood-brain barrier, could easily trigger an autoimmune response leading to a new attack of demyelination. If this occurs, antiviral agents might be effective in reducing the number of MS attacks.

There are possible alternative explanations for the increased incidence of both HSV and HHV-6 in MS brains, such as the relative immunosuppression seen with repeated steroid treatment and the use of other immunosuppressive agents that allow overgrowth of a pathogen normally present in brain. Since herpesviruses are frequently found in macrophages, the inflammatory response could itself be responsible. On the other hand, the presence of herpesviruses in the lesions would be expected, at the very least, to aggravate the inflammatory response and to increase the damage. Ex-

amination of the brains of patients with other inflammatory diseases of the central nervous system might help to clarify this issue.

While the possible involvement of herpesviruses has been suggested previously,[3-5] several outcomes can be anticipated from the recent observations discussed herein, eg, trials of drugs that are effective against herpesviruses, such as acyclovir, and even some of the more toxic ones, such as ganciclovir and foscarnet sodium. In fact, Lyke et al[6] described a pilot trial of acyclovir involving 30 patients, the results of which showed a 30% lower attack rate in the treated patients; however, because of the small size of the group, this did not reach statistical significance. An effort to develop a vaccine for roseola can also be anticipated. Additional polymerase chain reaction studies with identification of other viruses in other diseases may be expected and will present similar problems in interpretation. Some of those identified will undoubtedly be unrelated to the disease in question, since we all carry a number of viruses. Nevertheless, HHV-6 should be regarded as more than just another virus of the month in MS, and the relationship of herpesviruses to MS is deserving of serious further investigation.

Robert M. Herndon, MD
Portland, Ore

REFERENCES

1. Sanders VJ, Waddell AE, Felisan SL, Li X, Conrad AJ, Tourtellotte WW. Herpes simplex virus in postmortem multiple sclerosis brain tissue. *Arch Neurol.* 1996; 53:125.
2. Challoner PB, Smith KT, Parker JD, et al. Plaque-associated expression of human herpesvirus 6 in multiple sclerosis. *Proc Natl Acad Sci.* 1995;92:7440-7444.
3. Johnson RT. *Viral Infections of the Nervous System.* New York, NY: Raven Press; 1982.
4. Ellison GW. Multiple sclerosis: a fever blister on the brain. *Lancet.* 1974;2:664.
5. Nelson DA. Dorsal root ganglia may be reservoirs of viral infection in multiple sclerosis. *Med Hypotheses.* 1993;40:278-283.
6. Lyke J, Svennerholm BO, Hjelmqvist E, et al. Acyclovir treatment of relapsing-remitting multiple sclerosis: a randomized placebo controlled, double-blind study. In: Program and abstracts of the Multiple Sclerosis Satellite Symposium Following the 15th World Congress of Neurology; September 11-14, 1993; Victoria, British Columbia. Abstract 2-16.

STIC-ILL

From: Gambel, Phillip
Sent: Tuesday, July 23, 2002 4:00 PM
To: STIC-ILL
Subject: refernces of recrod in ussn 09 / 010377 rubin encephalitis

stic

please provide the following references to

phillip gambel
art unit 1644
308-3997

1644 mailbox 9E12

---

1) sanders et al. archives of neurology 53 : 125- 133 (1996)

2) editorial archives of neurology 53 : 123- 124 (1996)

3) soilo-hanninen et al. scand. j. immunol. 43 : 727 - ? (1996)

4) soilo-hanninen et al. j. neuroimmunol. 72 : 95 - 105 (1997)

5) planz et al. j. virol. 69 : 896 - 903 (1995)

thanx

404977

JOURNAL OF VIROLOGY, Feb. 1995, p. 896–903
0022-538X/95/$04.00+0

Vol. 69, No. 2

Immunopathogenic Role of T-Cell Subsets in Borna Disease Virus-Induced Progressive Encephalitis

OLIVER PLANZ,[1] THOMAS BILZER,[2] AND LOTHAR STITZ[1]*

Institut für Virologie, Justus-Liebig-Universität, Giessen,[1] and Institut für Neuropathologie, Heinrich-Heine-Universität, Düsseldorf,[2] Germany

Received 1 August 1994/Accepted 10 November 1994

Borna disease is an immunopathological virus-induced encephalopathy comprising severe inflammation and degenerative brain cell lesions which results in organ atrophy and chronic debility in rats. $CD4^+$ and $CD8^+$ T cells have been reported to be involved in the development of this disease of the central nervous system. A virus-specific homogeneous T-cell line, established in vitro after immunization of rats with the recombinant 24-kDa virus-specific protein, showed antigen-specific proliferation in the presence of the 24-kDa but not the 38-kDa Borna disease virus-specific protein, another major virus-specific antigen. This T-cell line, P205, was found to exhibit characteristics of a T-helper cell: $CD4^+$ $CD8^-$ IL-2$^-$ IL-4$^-$ IFN-γ^+ IL-6$^+$ IL-10$^+$. Furthermore, this T-cell line expressed the α/β T-cell receptor and the $\alpha 4$ integrin (VLA-4). Adoptive transfer of this helper cell resulted in an increase of antibody titers and two different types of disease in virus-infected rats after cyclophosphamide-induced immunosuppression. (i) Rats receiving T cells between 10 and 18 days after treatment with cyclophosphamide showed an acute lymphoproliferative disease in the gut and lungs within 9 days after adoptive transfer and died. (ii) Passive transfer within the first 5 days after immunosuppressive treatment resulted in typical Borna disease associated with neurological symptoms such as ataxia and paresis starting 14 to 16 days after transfer. Immunohistological analysis of the brains of rats with Borna disease uniformly revealed the presence of $CD8^+$ T cells in encephalitic lesions in addition to $CD4^+$ cells that were found in the brains of recipients of the virus-specific $CD4^+$ T-cell line, irrespective of whether neurological symptoms developed or not. However, recipient rats treated with antibodies against $CD8^+$ T cells developed neither encephalitis nor disease. Therefore, $CD4^+$ T cells appear to accumulate in the brain and cause perivascular inflammatory lesions which alone obviously do not cause disease. In contrast, the presence of $CD8^+$ cells apparently directly correlates with the development of neurological symptoms.

After infection of rats with Borna disease virus (BDV), a single-stranded RNA virus (9, 14), a central nervous system disease develops that finally results in brain atrophy and chronic debility (7, 8, 23, 32). The virus, which is tightly cell associated, lacks apparent cytopathogenicity in vitro (20), and there is only circumstantial evidence of in vivo cytopathogenicity (11). The virus replicates preferentially in cells derived from the neural crest such as neurons, astrocytes, and ependymal cells (11, 12, 15, 32); however, evidence of infection and an inflammatory response in the peripheral and autonomic nervous system has also recently been demonstrated (10, 12). The disease has been shown to be based on an immunopathological reaction (reviewed in reference 44) in which the cellular immune response, but not an antibody-mediated reaction to virus-specific antigens, results in severe encephalitis (21, 32, 48).

The original finding that $CD4^+$ T cells play a role in the development of the encephalitis was based on experiments with a $CD4^+$ T-cell line specific for a 38- to 39-kDa virus-specific protein (38, 39). This T-cell line showed some notable characteristics: adoptive transfer into cyclophosphamide (CY)-treated recipients between days 10 and 15 after immunosuppression resulted in death, or animals had to be killed in a moribund condition as early as 5 to 10 days after receiving the T cells. Furthermore, this cell line was found to lyse virus-infected target cells in vitro in a major histocompatibility complex (MHC) class II-restricted manner (37). More recent studies have revealed the involvement of $CD8^+$ T cells in Borna disease (BD) in rats (8, 35, 46, 47).

In the present report, we present for the first time the complete phenotypical and biological characterization of a BDV-specific $CD4^+$ T-cell line. The adoptive transfer of this 24 kDa protein-specific T cell line into virus-infected, CY-treated recipients resulted either in neurological disease with BD symptoms or in rapid death, dependent on whether the transfer occurred early or late after infection and immunosuppression, respectively. Rats that were treated with monoclonal antibodies (MAb) against $CD8^+$ cells and received the 24-kDa BDV protein-specific $CD4^+$ T-cell line did not show any clinical symptoms. These results support the view that both $CD4^+$ and $CD8^+$ T cells are operative in the pathogenic mechanism of BD and provide evidence that $CD8^+$ T cells are indispensable for BDV-induced immunopathology in the brain.

MATERIALS AND METHODS

Virus and experimental animals. Giessen strain He/80 of BDV was used throughout all studies. Five-week-old female Lewis rats were obtained from the Zentralinstitut für Versuchstierzucht, Hannover, Germany, and inoculated intracerebrally in the left hemisphere with 5×10^3 50% tissue culture-infective doses of BDV.

Propagation of the T-cell line. Lewis rats (8 to 10 weeks old) were immunized with 50 μg of a recombinant BDV-specific 24-kDa antigen (r24kd; reference 53) (kindly provided by H. Niemann, Tübingen, Germany) into both hind footpads. Twelve days later, the animals were anesthetized and popliteal lymph nodes were collected. Lymph nodes were minced, and lymphocytes were separated by Lympholyte R (Cedarlane, Hornsby, Ontario, Canada) gradient centrifugation. In a secondary in vitro restimulation, 5×10^6 cells were cultured in the presence of 30 μg of the r24kd antigen per ml together with the same number of irradiated syngeneic thymocytes. Thereafter, 5×10^7 lymphocytes were restimulated again with 5×10^6 irradiated syngeneic thymocytes and 30 μg of the r24kd antigen per

* Corresponding author. Mailing address: Institut für Virologie, Justus-Liebig-Universität, Frankfurter Str. 107, D-35392 Giessen, Germany. Phone: 49 6441 702 4993. Fax: 49 6441 32911. Electronic mail address: Lothar.Stitz@vetmed.uni-giessen.de.

ml for 4 days. Finally, the lymphocytes were cultured with 10% interleukin 2 (IL-2) supernatant-containing medium for 5 to 6 days before further restimulation with a specific antigen and syngeneic thymocytes, followed by cultivation again in the presence of IL-2. A BDV-specific antigen was also purified from the brains of infected rats by affinity chromatography by employing MAb (52) revealing the 38- and 24-kDa proteins.

Clinical evaluation. All experimental animals were examined daily and weighed, and disease symptoms were scored by two independent observers on an arbitrary scale of 0 to 3 based on the general state of health and the appearance of neurologic symptoms (scores: 1, slight uncoordination and fearfulness; 2, distinct ataxia or slight paresis; 3, paresis or paralysis). Body weight on the day of infection was defined as 100%, and the percentage of weight change was calculated.

Proliferation assay. T cells (5×10^4) were cultured in the presence of 5×10^5 irradiated syngeneic thymocytes and in the presence of 30 μg of the r24kd or r38kd (provided by W. I. Lipkin, Irvine, Calif.) BDV-specific protein per ml, influenza virus hemagglutinin, or vaccinia virus proteins or without antigen in flat-bottom 96-well microliter plates for 60 h. Thereafter, 0.2 μCi of [^{3}H]thymidine per well was added and after an additional 12 h the cells were collected and [^{3}H]thymidine incorporation was measured.

Reverse transcription-PCR analysis of lymphokine mRNA levels. For reverse transcription-PCR, total cellular RNA was isolated after CsCl gradient centrifugation from 10^7 cells of the r24kd-specific T-cell line and from several clones derived from this line. Magnetic beads (Dynabeads; Dianova, Hamburg, Germany) were used to separate the mRNA from the total cellular RNA as described by the manufacturer. RNA was reverse transcribed by using an oligo(dT) primer and murine leukemia virus reverse transcriptase before resuspension to a final volume of 20 μl. Reverse-transcribed mRNA was amplified in a 100-μl reaction volume containing 100 ng of each oligonucleotide primer per μl; 10 mM each dATP, dTTP, dGTP, and dCTP (Pharmacia, Freiburg, Germany); and 10 μl of a 10× buffer containing 500 mM KCl, 250 mM Tris-HCl (pH 8.3), 100 mM $MgCl_2$, and 5 U of ampli-Taq DNA polymerase (Amersham) per μl. The reaction was performed in a Biometra thermocycler for 35 cycles of 95°C for 1 min, 65°C for 2 min, and 72°C for 3 min with oligomers that amplify segments of 410 (IL-2), 378 (IL-4), 636 (IL-6), 284 (IL-10), 413 (gamma interferon [IFN-γ]), and 607 (β-actin) bp. Ten microliters was loaded onto a 2% agarose minigel and visualized by ethidium bromide staining.

Alternatively, nested reverse transcription-PCR was done for IL-2 and IL-4 to enhance the sensitivity of the amplification products (41). For this procedure, two consecutive PCRs, each involving 35 cycles of amplification, were utilized. For the first PCR an external pair of primers was used, while in the second PCR two nested primers were used which were internal to the first primer pair. The larger fragment produced by the first reaction was used as the template for the second PCR.

Hot-start PCR was performed in all cases. In this procedure, the polymerase was added after denaturation and preheating of the sample to 80°C to avoid nonspecific primer hybridization.

The following primers were used as described by Shankar et al. (40): external IL-2 sense, 5′-CATGTACAGCATGCAGCTCGCATCC-3′; external IL-2 antisense, 5′-CCACCACAGTTGCTGGCTCATCATC-3′; internal IL-2 sense, 5′-CAGGTGCTCCTGAGAGGGATCG-3′; internal IL-2 antisense, 5′-GAGCCC TTGGGGCTTACAAAAAG-3′; external IL-4 sense, 5′-TGATGGGTCTCAG CCCCCACCTTGC-3′; external IL-4 antisense, 5′-CTTTCAGTGTTGTGAGC GTGGACTC-3′; internal IL-4 sense, 5′-AACACCACGGAGAACGAGCTCA TC-3′; internal IL-4 antisense, 5′-AGTGAGTTCAGACCGCTGACACCT-3′; IL-6 sense, 5′-ATGAAGTTTCTCTCCGCAAGAGACTTCCAGCCAG-3′; IL-6 antisense, 5′-GTAGGTTTGCCGAGTAGACCTCATAGTGACC-3′ (the IL-10 primer was a gift from Ian Lipkin, University of California, Irvine [unpublished data]); β-actin sense, 5′-ATGCCATCCTGCGTCTGGACCTGGC-3′; β-actin antisense, 5′-AGCATTTGCGGTGCACGATGGAGGG-3′; IFN-γ sense, 5′-GTTACTGCCAAGGCACACTCATTGAAAGCC-3′; IFN-γ antisense, 5′-TCAGCACCGACTCCTTTTCCGCTTCCTTAGGC-3′.

Immunosuppression with CY or anti-T-cell MAb. One day after intracerebral BDV infection, the animals received 160 mg of CY per kg intraperitoneally (32). Alternatively, thymectomized rats were treated with 2 mg of purified mouse MAb directed against rat CD8$^+$ T cells (OX-8) or directed against all T cells (OX-52) 1 day before and 1 day after infection (47). After immunosuppression or antibody treatment, infected animals developed no signs of BD.

Adoptive transfer of the BDV-specific T-cell line. For adoptive-transfer studies, 10^6 to 10^7 activated cells of BDV-specific T-cell line P205 were injected intravenously after restimulation with the specific antigen and after 1 day of incubation in IL-2-containing medium at different time points after BDV infection.

Cytotoxicity assay. ^{51}Cr release assays were performed as previously described (35). Briefly, persistently infected syngeneic skin fibroblasts and an astrocytic cell line (F10; kindly provided by H. Wekerle, Munich, Germany) were treated with rat IFN-γ for 72 h to induce MHC class II expression. Target cells were labeled with 0.2 mCi of ^{51}Cr per 10^7 cells at 37°C for 1 h. P205 effector T cells and target cells were incubated at an effector-to-target cell ratio of 30:1 and at threefold dilutions of the original concentration of effector cells. After various periods of time (6 to 20 h), 50-μl samples were collected and counted in a gamma counter.

TABLE 1. Antigen-specific proliferation of CD4$^+$ T-cell line P205[a]

T-cell line	cpm of [^{3}H]thymidine incorporation (SI[b])					
	BDV antigen	r24kd	r38/39kd	HA[c]	VVP[d]	NS[e]
P205	16,663 (19)	22,948 (25)	2,294 (3)	1,554 (2)	1,062 (1)	877
Control	3,087 (21)	1,994 (14)	1,617 (11)	ND	ND	147

[a] Proliferation of P205 cells was tested after various restimulation cycles in the presence of a BDV-specific or irrelevant antigen. For details, see Materials and Methods. The control was a T-cell line induced by a mixture of native BDV-specific proteins and cultured in the presence of the same antigens. ND, not done.

[b] SI, stimulation index.

[c] HA, influenza virus type A hemagglutinin.

[d] VVP, vaccinia virus proteins.

[e] NS, no stimulation.

BDV-specific antibody measurement. BDV-specific antibodies were detected by an enzyme-linked immunosorbent assay method as previously described (48).

Histology and immunohistochemistry. Animals were killed at different time points after BDV infection. Brain tissue was either frozen in isopentane at −150°C or fixed in buffered paraformaldehyde. All tissue sections were stained with hematoxylin and eosin and with cresyl violet as described by Nissl. Encephalitic infiltrates were scored on an arbitrary scale of 0 to 3 based on the number of infiltrates per section and the number of cell layers in each infiltrate (scores: 1, up to 5 small infiltrates per section; 2, more than 5 small infiltrates per section or more than 3 infiltrates with multiple layers; 3, more than 10 small infiltrates or more than 5 infiltrates with multiple layers). Immunohistochemical analysis was carried out on cryostat sections to detect the presence of lymphocyte subsets and macrophages, as well as MHC antigens, IFN-γ, and tumor necrosis factor. The following MAbs (Serotec) were used: OX-8 for CD8$^+$ T cells, W3/25 and OX-38 for CD4$^+$ T cells, and ED1 for macrophages. The percentages of positive cells reactive with these MAb were determined by visual counting (8, 46).

Cytofluorometry. Unstained and stained P205 T cells were scanned on an Epics Elite laser flow cytometer (Coulter Electronics, Hialeah, Fla.). During data acquisition, the T-cell population was gated to exclude debris and 10^3 cells were counted per sample. Cells were incubated with various fluorescein isothiocyanate-conjugated MAb specific for leukocyte differentiation markers: W3/13 (T cells), OX-33 (B cells), W3/25 (CD4$^+$ T cells), and OX-8 (CD8$^+$ T cells) (Camon, Wiesbaden, Germany) and P12520 (VLA-4) and R73 (α/β T-cell receptor) (Dianova).

RESULTS

Induction and characterization of a BDV-specific 24-kDa T-cell line. Since the recombinant 24-kDa BDV-specific protein (r24kd) was used to induce T cells, we retested the immunologic relationship between the natural and recombinant 24-kDa proteins (53). Western blot (immunoblot) analysis and immunoprecipitation revealed the reactivity of both proteins with polyclonal BDV-specific antisera and MAb induced by either the native or the recombinant 24-kDa protein (data not shown). Popliteal lymph nodes obtained from rats immunized with the r24kd protein were removed, and lymphocytes were isolated and propagated in vitro. Numerous cycles of antigen-specific stimulation in the presence of irradiated syngeneic thymocytes and cultivation in IL-2-containing medium in the absence of virus-specific protein were carried out. To establish the antigen specificity of the T cells, proliferation assays were performed with native BDV-specific antigen purified either from the brains of BDV-infected rats by affinity chromatography or with recombinant proteins (Table 1). The results revealed antigen specificity for the r24kd protein compared with a T-cell line specific for the 38- or 39-kDa BDV-specific protein.

Furthermore, cultured r24kd-specific lymphocytes were analyzed for phenotypic markers in cytofluorometric assays. As shown in Fig. 1, the phenotype of the 24 kDa-specific lymphocytes is typical of CD4$^+$ T cells: W3/13$^+$ W3/25$^+$ OX-8$^-$ OX-33$^-$. The cell line was also found to carry the α/β T-cell re-

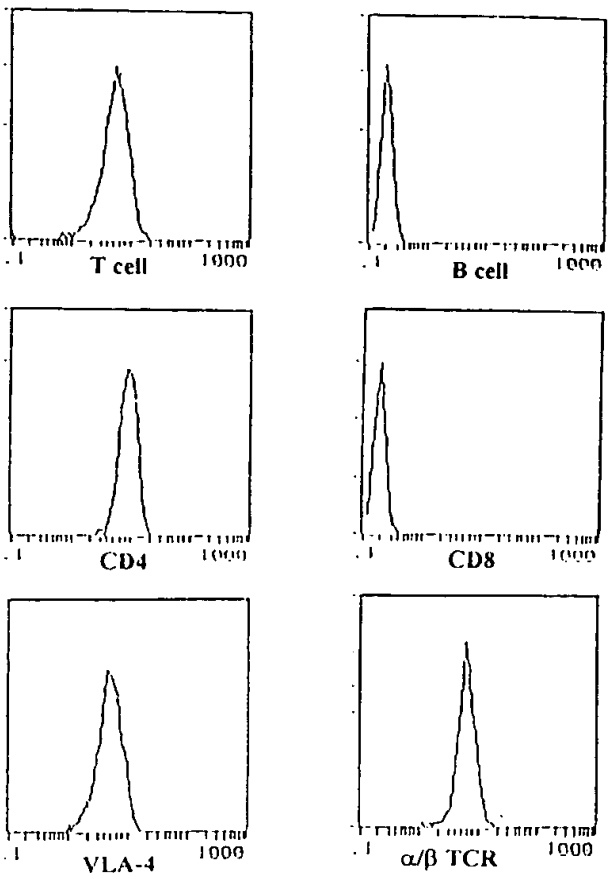

FIG. 1. Cytofluorographic histograms of T-cell line P205. The MAb used were W3/13 (T cells), OX-33 (B cells), W3/25 (CD4), OX-8 (CD8), PI2520 (VLA-4), and R73 (α/β T-cell receptor). For details, see Materials and Methods.

ceptor (MAb R73; reference 25) and express the VLA-4 (α4 integrin) molecule. This 24-kDa BDV-specific T-cell line is called P205.

To establish the cytokine profile, 10^7 cultured lymphocytes were lysed and RNA was extracted for reverse transcription-PCR. As shown in Fig. 2, PCR analyses revealed the presence

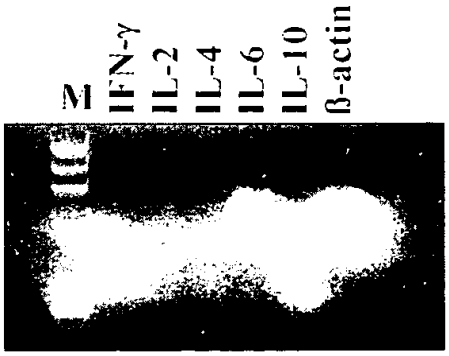

FIG. 2. PCR analyses of different cytokine mRNAs of CD4+ 24-kDa-specific T-cell line P205. Lane M, molecular size markers (ϕX174 digested with *Hae*III). For further details, see Materials and Methods.

TABLE 2. Effect of adoptive transfer of the P205 BDV-specific T-cell line on antiviral antibody synthesis[a]

Expt	CY treatment	Transfer	BDV-specific antibody titer		
			Day 10 p.i.	Day 13 p.i.	Day 24 p.i.
Control	−	−	<1:40	1:80	>1:5,120
1A	−	+	1:160	1:320	>1:5,120
2A	−	+	1:320	1:1,280	>1:5,120
3A	−	+	1:40	1:80	ND
Control	+	−	<1:40	<1:40	<1:40
1B	+	+	<1:40	<1:40	1:80
2B	+	+	<1:40	<1:40	1:160

[a] BDV-infected, untreated (CY$^-$) and BDV-infected, CY-treated, immunosuppressed (CY$^+$) rats received 2.5×10^6 (experiments 1A and 2A and 1B and 2B) or 2.5×10^5 (experiment 3A) P205 CD4$^+$ T cells, and serum antibody titers were measured at different time points with an enzyme-linked immunosorbent assay. The antibody titers given represent the means of three animals. Titer variations never exceeded one level. ND, not done.

of mRNAs specific for IL-6, IL-10, and IFN-γ, whereas no reaction was found with oligonucleotide primers for IL-2 and IL-4.

The cytotoxic activity of the P205 cell line was tested on syngeneic BDV-infected fibroblasts and astrocytes. Infected astrocyte target cells were pretreated with IFN-γ for 72 h to induce MHC class II antigen expression (59). Cytofluorometric analysis and indirect immunofluorescence revealed the presence of MHC class II antigen on BDV-infected astrocytic cells but not on fibroblasts (data not shown) as described earlier (35, 37). Neither MHC class I-positive fibroblast nor MHC class II-positive astrocyte target cells were lysed; in addition, P205 cells did not exert natural killer activity since NK-sensitive YAC-1 target cells were not lysed (data not shown).

T-helper activity of BDV-specific CD4$^+$ T-cell line P205. To determine whether the P205 cell line exerts helper activity in vivo, adoptive-transfer experiments were carried out with BDV-infected rats. Activated P205 cells were adoptively transferred into BDV-infected, untreated rats or infected and then CY-treated recipients (Table 2).

BDV-infected, not immunosuppressed recipients of 2.5×10^6 P205 T cells showed antiviral antibodies as early as 5 days posttransfer (p.t.), i.e., 10 days postinfection (p.i.), whereas infected but otherwise untreated control animals had no detectable antibodies at this time point (Table 2, experiments 1A and 2A). At day 8 p.t. (day 13 p.i.), the antibody titers of rats having received P205 cells had further increased compared with those of infected, untreated rats, in which low antibody titers were detected only after day 12 p.i. (Table 2, experiments 1A to 3A). Antibody titers directly correlated with the number of cells transferred: transfer of 2.5×10^6 cells (experiments 1A and 2A) resulted in two- to fourfold higher antibody titers than did transfer of 2.5×10^5 cells (experiment 3A).

Because of the immunosuppressive effect of CY, animals treated with CY 1 day after BDV infection did not synthesize detectable antiviral antibodies (Table 2, experiments 1B and 2B). After passive transfer of P205 T cells, however, antibodies specific for BDV were detected at day 19 p.t. (day 24 p.i.) (Table 2, experiments 1B and 2B). Thus, rat T-cell line P205 shows characteristics of a functional T-helper cell line.

Induction of immunopathological disease after adoptive transfer of BDV-specific CD4$^+$ T-cell line P205. Passive transfer of P205 T cells into normal or CY-treated, uninfected recipients resulted in neither pathological brain alterations nor clinical signs, providing evidence that this T-cell line is not encephalitogenic (data not shown).

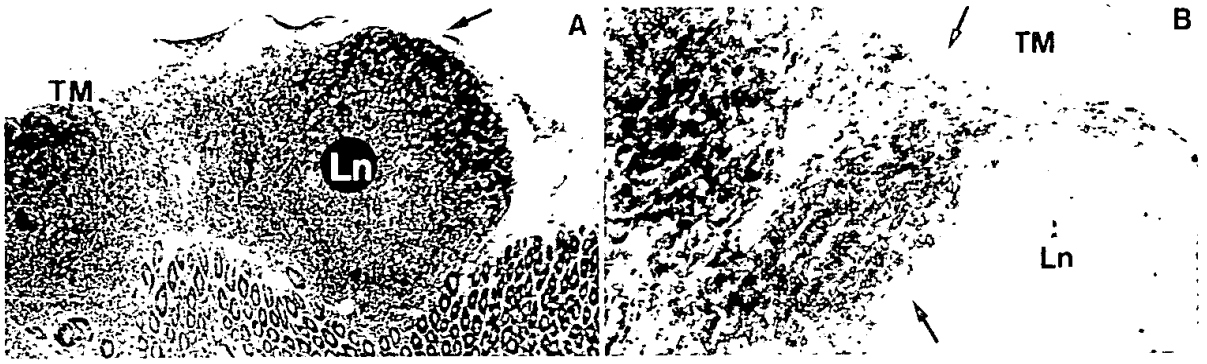

FIG. 3. Severe lymphocellular proliferation in Peyer's patches and diffuse proliferation within the intestinal wall in a BDV-infected immunosuppressed rat subjected to adoptive transfer of $CD4^+$ T-cell line P205 at day 10 after CY treatment. (A) Lymphocytic infiltration extends from the epithelial layer (lamina epithelialis) into the muscular layer (tunica muscularis), which is markedly reduced in size (arrow). Staining was done with hematoxylin and eosin. Magnification, ×50. (B) Immunohistochemical analysis of a corresponding slide with MAb OX-38 showing that most of the diffusely infiltrating cells outside the nodule are CD4 positive (arrows). TM, tunica muscularis; Ln, solitary lymph nodule. Immunohistochemical staining was done by the ABC method. Magnification, ×80.

Transfer of activated P205 T cells into BDV-infected, immunosuppressed rats resulted in two different pattern of disease dependent on the time of transfer relative to the time point after CY treatment.

(i) Late transfer. Late transfer of 10^6 to 10^7 P205 cells on day 10 or 15 after immunosuppression resulted in a drastic weight loss starting immediately after injection (Fig. 4). All rats receiving 10^7 or 10^6 P205 cells died within 7 to 9 days after transfer without developing neurological symptoms. Quantitation of brain lymphocytes was not done because of the low encephalitis scores, irrespective of the fact that both T-cell subpopulations were identified immunohistochemically. In the periphery, i.e., the lungs and intestines, most (>70%) of the lymphocytes were $CD4^+$ (Table 3).

Histological examination of the brains of BDV-infected, immunosuppressed recipients of P205 T cells revealed only moderate encephalitis, which did not correlate with their general bad health. Macroscopically, the entire intestine, including the mesenteric lymph nodes, showed signs of severe lymphoproliferative disease, i.e., many nodules in the intestinal wall and the regional lymph nodes. Histologically, a massive lymphocytic infiltration was found in the intestinal wall, in mesenteric lymph nodes, in Peyer's patches, and in the lungs of BDV-infected rats having received the BDV-specific T-cell line later than 10 days after immunosuppression (Fig. 3A). Immunohistological characterization of infiltrating cells revealed the majority of the lymphocytes diffusely infiltrating the intestinal wall to be CD4 positive (Fig. 3B). Animals receiving 10^5 cells and uninfected rats receiving the highest number of $CD4^+$ T cells showed normal weight gain and no clinical symptoms throughout an observation period of 100 days (data not shown).

(ii) Early transfer. Early transfer of P205 T cells 4 days after immunosuppression resulted in disease symptoms comparable to those of infected but otherwise untreated rats. By day 12 p.t., recipient rats showed moderate weight loss (Fig. 4), ruffled fur, and hunched backs. Neurological symptoms such as slight ataxia were first detectable at day 14 p.t. and increased during the next few days, resulting in paresis and, in some cases, paralysis by day 18 or 19 p.t. (Table 4). One rat died on day 19 p.t., but otherwise all other animals were killed on the same day because of their bad health. Macroscopical and histological examination of lymph nodes, intestines, and lungs did not reveal any significant cellular infiltration. In the brain, however, severe encephalitic reactions on day 14 that increased until day 19 were observed (Fig. 5).

Immunohistologically, more than 50% of the inflammatory cells were $CD4^+$ T cells and about 20% of T cells in perivascular infiltrations and about 30 to 40% of T cells in parenchymal infiltrations were CD8 positive (Fig. 5). BDV-infected, CY-treated controls which had not received T cells showed neither encephalitic lesions nor disease (data not shown).

Absence of immunopathological disease after transfer of cell line P205 into anti-T-cell antibody-treated recipients. Experiments similar to those described above were carried out with thymectomized rats which had been treated with MAb OX-8 (directed against $CD8^+$ cells) or OX-52 (directed against all T cells). Rats treated in this way have been shown to stay healthy after BDV infection (47). Adoptive transfer of as many as 5 ×

TABLE 3. Effect of transfer of P205 $CD4^+$ T-cell line into BDV-infected recipients late after CY immunosuppression[a]

No. of cells transferred	Outcome	Day p.t.	Encephalitis		T cells present in:		Body wt change (%)
			No. of rats with encephalitis/total	Mean score ± SEM	Brain[b]	Lungs, intestines[c]	
10^7	6 of 6 dead	7	3/6	0.4 ± 0.5[d]	CD4, CD8	CD4	−29
10^6	6 of 6 dead	9	4/6	0.5 ± 0.8[e]	CD4, CD8	CD4	−28
10^5	6 of 6 killed	28	2/6	0.3 ± 0.3[f]	CD4, CD8	CD4	−4

[a] Recipient rats were subjected to adoptive transfer of the indicated numbers of P205 T cells on day 10 p.t., i.e., day 9 after CY immunosuppression.
[b] Quantitation of brain lymphocytes was not done because of the low encephalitis scores.
[c] More than 70% of lymphocytes were $CD4^+$; $CD8^+$ cells were not found.
[d] The individual scores were 0, 0, 0, 0.5, 0.5, and 1.5.
[e] The individual scores were 0, 0, 0, 0, 1.5, and 1.5.
[f] The individual scores were 0, 0, 0.5, 0.5, 0.5, and 0.5.

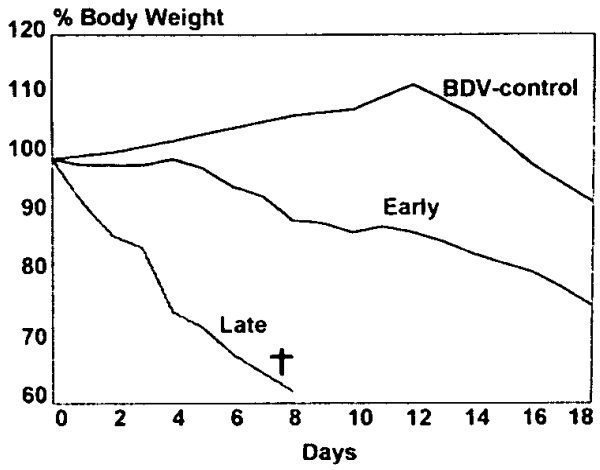

FIG. 4. Growth curves of BDV-infected, CY-treated rats receiving adoptive transfer of P205 T cells late (Late) or early (Early) after immunosuppression and of untreated, BDV-infected control animals (BDV-control). Day zero was the day of cell transfer (Early and Late) or BDV infection (BDV-control). †, death.

10^6 $CD4^+$ P205 T cells, which caused encephalitis and BD in CY-treated rats, did not cause weight loss, clinical symptoms, or inflammation of the brain (Table 5). In contrast, antibody-treated rats receiving immune spleen cells from BDV-infected donors showed BD symptoms and had encephalitis.

Histological examination revealed the presence of few inflammatory cells in the brain, as well as in the lungs and liver (data not shown). A slight cellular infiltration was also observed in OX-8-treated control rats (Table 5) which had not received $CD4^+$ T-cell passive transfer. This phenomenon has been observed earlier (47) and immunohistological examination of infiltrates revealed the presence of $CD4^+$ T cells and macrophages but not that of $CD8^+$ T cells in antibody-treated rats (8).

DISCUSSION

Adoptive transfer of a $CD4^+$ T-cell line specific for the 24-kDa BDV antigen into virus-infected and CY-immunosuppressed rats results in either death within a few days or BD-associated neurological symptoms. Transfer of the cell line into infected rats which had been treated with MAb directed against $CD8^+$ or all T cells did not result in disease. Passive transfer also revealed enhanced kinetics of antiviral antibody synthesis. In addition to the phenotypic characterization, PCR analysis of the T-cell line revealed a cytokine pattern indicative of T-helper cells. No cytotoxic activity was found on MHC class II-matched virus-infected and IFN-γ-treated target cells or on NK-sensitive YAC-1 cells.

We have previously shown that $CD8^+$ T cells are an integral component of the immunopathological reaction in BD (reviewed in reference 45). The role of $CD4^+$ T cells in BD has been demonstrated earlier in experiments with a $CD4^+$ T-cell line specific for the 38- to 39-kDa antigen (reviewed in reference 44).

Since $CD8^+$ T cells generally have never been successfully established as lines or clones from rats, in this report we have reviewed the importance of $CD4^+$ T cells in BD in view of our recent reports on the role of $CD8^+$ T cells. Therefore, a homogeneous 24-kDa virus-specific $CD4^+$ T-cell line was generated. This noncytotoxic T-cell line and derived clones (data not shown) exhibit a helper cytokine profile and enhance the immunoglobulin response; hence, they are functional helper T cells. The characteristics suggest the presence of an intermediate or unusual phenotype of T-helper cells (17, 31a, 34, 36).

The most interesting feature of P205 T cells is the impact on the cell-mediated immune reaction after transfer. Experiments presented in this communication revealed two different patterns of disease, dependent on the time of transfer after CY treatment. When transfer of T cells was carried out at late time points after the initial immunosuppression, i.e., 10 to 15 days after CY, recipients died within 7 to 9 days without neurological symptoms but with a drastic loss of body weight of up to 30% within 3 days. Macroscopical and histological examination revealed signs of a severe lymphoproliferative disease of the

TABLE 5. Adoptive transfer of P205 $CD4^+$ T-cell line into anti-T-cell MAb-treated, BDV-infected recipients[a]

MAb	Cells transferred	Encephalitis		Body wt change (%)
		No. of rats with disease/total	Mean score ± SEM	
OX-8	P205	0/4	0	+>30
OX-8	None	1/4	0.1 ± 0.25[b]	+>30
OX-8	Immune spleen	4/4	2.4 ± 0.3[c]	−15
OX-52	P205	0/4	0	+>30
OX-52	None	0/4	0	+>30
OX-52	Immune spleen	4/4	2.5 ± 0.4[d]	−18

[a] Recipient rats were subjected to adoptive transfer of 5×10^6 P205 T cells or 10^7 spleen cells from diseased BDV-infected donors. Recipients were treated with MAb OX-8 (directed against $CD8^+$ cells) or OX-52 (directed against all T cells) on days −1 and −1 relative to the day of infection. The cells were transferred on day 21 p.i.

[b] The individual scores were 0, 0, 0, and 0.5.

[c] The individual scores were 2.0, 2.5, 2.5, and 2.5.

[d] The individual scores were 2.0, 2.5, 2.5, and 3.0.

TABLE 4. Effect of early transfer of P205 $CD4^+$ T-cell line into BDV-infected recipients[a]

No. of cells transferred	No. of rats with symptoms/total	Day p.t.	Encephalitis		T cells present in:		Body wt change (%)
			No. of rats with encephalitis/total	Mean score ± SEM	Brain	Lungs, intestines	
10^6	6/6	14	6/6	1.5 ± 0.4[b]	CD4, CD8	None	−23
10^6	6/6	16	6/6	1.75 ± 0.3[c]	CD4, CD8	None	−30
10^6	6/6	19	6/6	2.0 ± 0.4[d]	CD4, CD8	None	−29

[a] Recipient rats were subjected to adoptive transfer of 10^6 P205 T cells on day 5 p.i., i.e., day 4 after CY immunosuppression, and killed at various time points thereafter.

[b] The individual scores were 1.0, 1.5, 1.5, 1.5, 1.5, and 2.0.

[c] The individual scores were 1.0, 1.5, 1.5, 2.0, 2.0, and 2.0.

[d] The individual scores were 1.5, 1.5, 2.0, 2.0, 2.5, and 2.5.

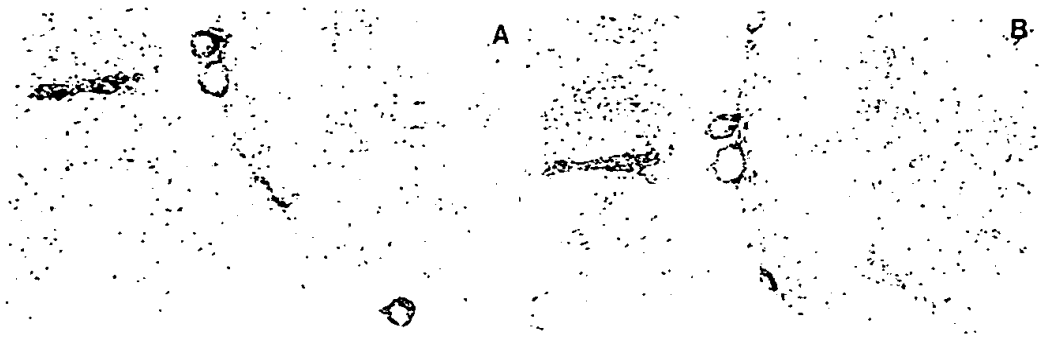

FIG. 5. Hippocampus region in the brain of a BDV-infected, immunosuppressed rat subjected to adoptive transfer of $CD4^+$ T-cell line P205 at day 4 after CY treatment. The presence of $CD4^+$ (A) and $CD8^+$ (B) cells as detected by MAb W3/25 and OX-8, respectively, is shown. Immunohistochemical staining was done by the ABC method. Magnification, ×80.

lungs, mesenteric lymph nodes, intestinal wall, and Peyer's patches. Since T cells in general and activated T-helper cells in particular are potent producers of cytokines and since transferred T cells, including virus-specific lymphocytes, preferentially migrate through the lungs and to the lymphoid tissue of the gut (4, 18, 19, 43, 55), it is likely that the observed inflammatory disease in peripheral organs is initiated by these cells. Interestingly, no BDV-specific antigen was found at this time in the guts or lungs of recipient rats. Therefore, we anticipate that transferred activated T-helper cells induce a fast and vehement but rather unspecific local immune response due to their cytokine synthesis and subsequent infiltration of other cell types into the reactive tissue. Migration of inflammatory cells into these areas is possible because the immune system has recovered, at the latest, by day 10 after CY treatment, when the adoptive transfer occurred. Cytofluorometric analyses of mesenteric lymph nodes revealed the presence of $CD4^+$ and $CD8^+$ cells 10 days after CY treatment; numbers and staining intensities of cells were comparable to those of cells from untreated rats, providing evidence of rather quick recovery of the immune system from the suppressive effects of CY (data not shown). In the brains of these rats, only slight inflammatory reactions were observed which, according to our experience, could probably not have caused rapid death without neurological symptoms. Therefore, we argue that the massive inflammation, especially in the intestines, caused the death of recipients before a BDV-specific immune response was generated in the brain.

In contrast, transfer of P205 $CD4^+$ T cells shortly after CY treatment, when the immunosuppressive effect does not allow sudden induction of a cellular host reaction because of the absence of lymphocytes, led to full-blown BD. In this case, in contrast to adoptive transfer late after CY immunosuppression, transferred T cells may be redistributed and finally migrate to the brain. In this respect, it is of importance that P205 T cells express the α4 integrin (VLA-4) which has been shown to be the crucial molecule that allows entry of activated T cells into the brain after binding to VCAM-1 on endothelial cells (5, 22, 57). In rats that received a passive transfer shortly after CY treatment, disease started around day 14 p.t. with a moderate loss of body weight and gradual development of neurological symptoms within the next few days resulting in ataxia and pareses. Immunohistochemical characterization of inflammatory cells in the brains of recipients of $CD4^+$ P205 T cells unanimously revealed the presence of about 20 to 30% $CD8^+$ T cells and more than 50% $CD4^+$ T cells with respect to the total number of lymphocytes.

In sharp contrast, recipients which had been thymectomized and treated with MAb against $CD8^+$ (OX-8) or all (OX-52) T cells prior to the transfer of P205 T cells did not show disease symptoms or notable encephalitic reactions (8, 47).

Recently, increasing evidence of the pathogenic importance of $CD8^+$ T cells in organ diseases has been presented. A wide body of evidence in favor of the activity of $CD8^+$ T cells in other virus infections of the brain has also been presented. In lymphocytic choriomeningitis virus, herpes simplex virus, West Nile virus, and Theiler's virus infections in mice (24, 30, 31, 33, 61); human immunodeficiency virus and human T-cell leukemia virus infections in humans; and Visna virus infections in sheep, $CD8^+$ cytotoxic T lymphocytes have been shown or are suspected to be a deleterious factor in the disease and/or to contribute to neurological disorders (16, 26, 27, 41, 49, 54, 56, 58).

Our own observations revealed that the presence of functional $CD8^+$ T cells in the brains of BDV-infected rats was paralleled by development of neurological disease, upregulation of MHC class I antigen in the brain, and MHC class I-restricted virus-specific cytotoxic activity in vitro (8, 35, 46, 47). Perivascular inflammations in BD encephalitis, in addition to macrophages, are predominantly composed of $CD4^+$ T cells of which the majority might be antigen-nonspecific, host-derived cells, as it has been shown in other models (1, 2, 13), since their presence, in the absence of $CD8^+$ T cells in parenchymal and perivascular infiltrations, has no pathological impact (8, 46, 47); furthermore, despite the high numbers of $CD4^+$ T cells in the brain (15, 38, 46), no considerable MHC class II-restricted killing, compared with high MHC class I-restricted lysis, was found in lymphocyte preparations isolated from the brains of BDV-infected rats (35). Finally, IFN-γ, which is secreted by cytotoxic T lymphocytes (34, 50) after they encounter their antigen in vivo, has also been detected in the brains of rats with BD (40). This cytokine activates macrophages and induces a delayed-type hypersensitivity reaction—in part from nonspecific host inflammatory cells—that finally results in tissue injury. In this context, it is of interest that both Th1 and Th2 cells have been shown to provide help to cytotoxic T lymphocytes and trigger production of IFN-γ by cytotoxic T lymphocytes (51). Since BDV is a noncytopathic virus that by itself does not cause detectable destruction in vitro or in vivo (20, 32), the cytotoxic T-cell response appears to be a major pathway to release of virus-specific antigen from infected cells, which might lead to promotion of the immune response, including induction of $CD4^+$ T cells. Our earlier and present observations on BD demonstrate that different types of $CD4^+$

T cells can be induced, represented by $CD4^+$ T-cell line NM1, which apparently has direct pathological effects (38, 39), and by $CD4^+$ T-cell line P205, which provides help. Therefore, these two different T-cell lines and their different in vivo effects upon adoptive transfer might reflect the broad spectrum of $CD4^+$ T cells found in vivo.

In conclusion, this work employing a T-helper cell line specific for a major BDV antigen provides additional evidence of the importance of virus-specific $CD8^+$ T cells in BDV-induced encephalitis that results in brain atrophy and chronic debility. As demonstrated also in other virus infections, virus-specific $CD4^+$ T cells apparently act as helpers and contribute to the immune reaction on the T- and B-cell level. Dependent on the virus studied, in vivo experiments have revealed a mandatory role for T help in the induction of a cytotoxic T-cell response in some viral infections (3, 6, 28, 29, 60). Our findings support the notion that actions of CD4 and CD8 subsets are required for antiviral delayed-type hypersensitivity responses. BD in rats appears to be a $CD4^+$ T-cell-dependent immunopathological disease in which $CD8^+$ T cells and/or $CD8^+$ T-cell-mediated cytodestructive mechanisms are operative.

ACKNOWLEDGMENTS

We thank Rudolf Rott for encouragement, support, and hospitality; Martin Sobbe for MAb treatment of rats; and Silke Gommel for outstanding technical assistance. Ian Lipkin and Heiner Niemann kindly provided recombinant virus proteins.

This work was supported by the Deutsche Forschungsgemeinschaft (DFG-Forschergruppe "Pathogenitätsmechanismen von Viren," Sti 71/2-1 and Bi-323/2-2) and the EC Network "Pathogenesis of subacute and chronic inflammatory diseases of the central nervous system." L. Stitz is a recipient of a Hermann and Lilly Schilling Professorship for Theoretical and Clinical Medicine.

REFERENCES

1. **Ando, K., L. G. Guidotti, S. Wirth, T. Ishikawa, G. Missale, T. Moriyama, R. D. Schreiber, H.-J. Schlicht, S. Huang, and F. V. Chisari.** 1994. Class I-restricted cytotoxic T lymphocytes are directly cytopathic for their target cells in vivo. J. Immunol. 152:3245–3253.
2. **Ando, K., T. Moriyama, L. G. Guidotti, S. Wirth, R. D. Schreiber, H. J. Schlicht, S. Huang, and F. V. Chisari.** 1993. Mechanisms of class I restricted immunopathology. A transgenic mouse model of fulminant hepatitis. J. Exp. Med. 178:1541–1554.
3. **Ashman, R. B., and A. Müllbacher.** 1979. A T helper cell for anti-viral cytotoxic T cell responses. J. Exp. Med. 150:1277–1282.
4. **Baenziger, J., H. Hengartner, R. M. Zinkernagel, and G. A. Cole.** 1986. Induction or prevention of immunopathological disease by cloned cytotoxic T cell lines specific for lymphocytic choriomeningitis virus. Eur. J. Immunol. 16:387–393.
5. **Baron, J. L., J. A. Madri, N. H. Ruddle, G. Hashim, and C. A. Janeway, Jr.** 1993. Surface expression of α4 integrin by CD4 T cells is required for their entry into brain parenchyma. J. Exp. Med. 177:57–68.
6. **Bennink, J. R., and P. C. Doherty.** 1978. Different rules govern help for cytotoxic T cells and B cells. Nature (London) 276:829–831.
7. **Bilzer, T., and L. Stitz.** 1993. Brain cell lesions in Borna disease are mediated by T cells. Arch. Virol. Suppl. 7:153–158.
8. **Bilzer, T., and L. Stitz.** 1994. Immune-mediated brain atrophy. $CD8^+$ T cells contribute to tissue destruction during Borna disease. J. Immunol. 153:818–823.
9. **Briese, T., J. C. de la Torre, A. Lewis, H. Ludwig, and W. I. Lipkin.** 1992. Borna disease virus, a negative-strand RNA virus, transcribes in the nucleus of infected cells. Proc. Natl. Acad. Sci. USA 89:1186–1189.
10. **Carbone, K. M., C. S. Duchala, J. W. Griffin, A. L. Kincaid, and O. Narayan.** 1987. Pathogenesis of Borna disease in rats: evidence that intra-axonal spread is the major route for virus dissemination and the determinant for disease incubation. J. Virol. 61:3431–3440.
11. **Carbone, K. M., S. W. Park, S. A. Rubin, R. W. Waltrip, and G. B. Vogelsang.** 1991. Borna disease: association with a maturation defect in the cellular immune response. J. Virol. 65:6154–6164.
12. **Carbone, K. M., B. D. Trapp, J. W. Griffin, C. S. Duchala, and O. Narayan.** 1989. Astrocytes and Schwann cells are virus-host cells in the nervous system of rats with Borna disease. J. Neuropathol. Exp. Neurol. 48:631–644.
13. **Cohen, J. A., D. M. Essayan, B. Zweiman, and R. P. Lisak.** 1987. Limiting dilution analysis of the frequency of antigen reactive lymphocytes isolated from the central nervous system of Lewis rats with experimental allergic encephalomyelitis. Cell. Immunol. 108:203–213.
14. **de la Torre, J. C., K. M. Carbone, and W. I. Lipkin.** 1990. Molecular characterization of Borna disease agent. Virology 179:853–856.
15. **Deschl, U., L. Stitz, S. Herzog, K. Frese, and R. Rott.** 1990. Determination of immune cells and expression of major histocompatibility complex class II antigen in encephalitic lesions of experimental Borna disease. Acta Neuropathol. 81:41–50.
16. **Elovaara, I., S. Koenig, A. Y. Brewah, R. M. Woods, T. Lehky, and S. Jacobson.** 1993. High human T cell lymphotropic virus type 1 (HTLV-1)-specific precursor cytotoxic T lymphocyte frequencies in patients with HTLV-1-associated neurological disease. J. Exp. Med. 177:1567–1573.
17. **Firestein, G. S., W. D. Roeder, J. A. Laxer, K. S. Townsend, C. T. Weaver, J. T. Horn, J. Linton, B. E. Torbett, and A. L. Glasebrook.** 1989. A new murine $CD4^+$ T cell subset with an unrestricted cytokine profile. J. Immunol. 143:518–524.
18. **Gowans, J. L., and E. J. Knight.** 1964. The route of recirculation of lymphocytes in the rat. Proc. R. Soc. Lond. B Biol. Sci. 159:257–282.
19. **Hamann, A., and D. Jablonski-Westrich.** 1993. Integrins and L-selectin in lymphocyte endothelium interactions and homing into gut-associated tissue. Behring Inst. Mitt. 92:30–35.
20. **Herzog, S., and R. Rott.** 1980. Replication of Borna disease virus in cell culture. Med. Microbiol. Immunol. 168:153–158.
21. **Herzog, S., K. Wonigeit, K. Frese, H. J. Hedrich, and R. Rott.** 1985. Effect of Borna disease virus infection in athymic rats. J. Gen. Virol. 66:503–508.
22. **Hickey, W. F., B. L. Hsu, and H. Kimura.** 1991. T-lymphocyte entry into the central nervous system. J. Neurosci. Res. 28:254–260.
23. **Hirano, N., M. Kao, and H. Ludwig.** 1983. Persistent, tolerant and subacute infection in Borna disease virus infected rats. J. Gen. Virol. 64:305–315.
24. **Hudson, S. J., and J. W. Streilein.** 1994. Functional cytotoxic T cells are associated with focal lesions in the brain of SJL mice with experimental herpes simplex encephalitis. J. Immunol. 152:5540–5547.
25. **Hünig, T., H. J. Walloy, J. K. Hartley, A. Lawthky, and G. Tiefenthaler.** 1989. A monoclonal antibody to a constant determinant of the rat T-cell antigen receptor that induces T cell-activation: differential reactivity with subsets of immature and mature T lymphocytes. J. Exp. Med. 169:73–82.
26. **Jacobson, S., H. Shida, D. E. McFarlin, A. S. Fauci, and S. Koenig.** 1991. Circulating $CD8^+$ cytotoxic T lymphocytes specific for HTLV-I pX in patients with HTLV-I associated neurological disease. Nature (London) 348: 245–248.
27. **Jassoy, C., R. P. Johnson, B. A. Navia, J. Worth, and B. D. Walker.** 1992. Detection of vigorous HIV-1-specific cytotoxic T lymphocyte response in cerebrospinal fluid from infected persons with AIDS dementia complex. J. Immunol. 149:3113–3119.
28. **Kast, W. M., A. M. Bronkhorst, L. P. DeWaal, and C. J. M. Melief.** 1986. Cooperation between cytotoxic and helper T lymphocytes in protection against lethal Sendai virus infection: protection by T cells is MHC-restricted and MHC-regulated; a model for MHC-disease associations. J. Exp. Med. 164:723–738.
29. **Leist, T. P., M. Kohler, and R. M. Zinkernagel.** 1989. Impaired generation of antiviral cytotoxicity against lymphocytic choriomeningitis and vaccinia virus in mice treated with CD4-specific monoclonal antibody. Scand. J. Immunol. 30:679–686.
30. **Lindsley, M. D., R. Thiemann, and M. Rodriguez.** 1991. Cytotoxic T cells isolated from the central nervous system of mice infected with Theiler's virus. J. Virol. 65:6612–6618.
31. **Liu, Y., R. V. Blanden, and A. Müllbacher.** 1989. Identification of cytolytic lymphocytes in West Nile virus-infected murine central nervous system. J. Gen. Virol. 70:565–573.

31a. **Mosmann, T. R., J. H. Schumacher, N. F. Street, R. Budd, A. O'Garra, T. A. Fong, M. W. Bond, K. W. M. Moore, A. Sher, and D. F. Fiorentino.** 1991. Diversity of cytokine synthesis and function of mouse $CD4^+$ T cells. Immunol. Rev. 123:209–221.

32. **Narayan, O., S. Herzog, K. Frese, K. Scheefers, and R. Rott.** 1983. Pathogenesis of Borna disease in rats: immune-mediated viral ophthalmoencephalopathy causing blindness and behavioral abnormalities. J. Infect. Dis. 148: 305–315.
33. **Oldstone, M. B. A.** 1987. Immunotherapy for virus infection, p. 211–229. *In* M. B. A. Oldstone (ed.), Arenaviruses: biology and immunotherapy. Springer Verlag KG, Berlin.
34. **Paliard, X., R. D. Malefijt, H. Yssel, D. Blanchard, I. Chretien, J. Abrams, J. E. de Vries, and H. Spits.** 1988. Simultaneous production of IL-2, IL-4, and IFN-γ by activated human $CD4^+$ and $CD8^+$ T cell clones. J. Immunol. 141:849–855.
35. **Planz, O., T. Bilzer, M. Sobbe, and L. Stitz.** 1993. Lysis of MHC class I-bearing cells in Borna disease virus-induced degenerative encephalopathy. J. Exp. Med. 178:163–174.
36. **Powrie, F., D. Fowell, A. J. McKnight, and D. Mason.** 1991. Lineage relationships and functions of $CD4^+$ T-cell subsets in the rat. Res. Immunol. 142:54–58.
37. **Richt, J. A., and L. Stitz.** 1992. Borna disease virus infected astrocytes function in vitro as antigen-presenting and target cells for virus-specific

CD4-bearing lymphocytes. Arch. Virol. 124:95–109.
38. **Richt, J. A., L. Stitz, U. Deschl, K. Frese, and R. Rott.** 1990. Borna disease virus-induced meningoencephalomyelitis caused by a virus-specific CD4+ T-cell mediated immune reaction. J. Gen. Virol. 71:2565–2573.
39. **Richt, J. A., L. Stitz, H. Wekerle, and R. Rott.** 1989. Borna disease, a progressive meningoencephalomyelitis as a model for CD4+ T cell-mediated immunopathology in the brain. J. Exp. Med. 170:1045–1050.
40. **Shankar, V., M. Kao, A. N. Hamir, H. Sheng, H. Koprowski, and B. Dietzschold.** 1992. Kinetics of virus spread and change in levels of several cytokine mRNAs in the brain after intranasal infection of rats with Borna disease virus. J. Virol. 66:992–998.
41. **Simmonds, P., P. Balfe, J. F. Peutherer, C. A. Ludlam, J. O. Bishop, and A. J. L. Brown.** 1990. Human immunodeficiency virus-infected individuals contain provirus in small numbers of peripheral mononuclear cells and at low copy numbers. J. Virol. 64:864–870.
42. **Skias, D., D.-K. Kim, A. Reder, J. Antel, D. Lancki, and F. Fitch.** 1987. Susceptibility of astrocytes to class I MHC antigen-specific cytotoxicity. J. Immunol. 138:3254–3260.
43. **Smith, M. E., and W. L. Ford.** 1983. The recirculating lymphocyte pool of the rat: a systematic description of the migration behaviour of recirculating lymphocytes. Immunology 49:83–94.
44. **Stitz, L., T. Bilzer, J. A. Richt, and R. Rott.** 1993. Pathogenesis of Borna disease. Arch. Virol. Suppl. 7:135–151.
45. **Stitz, L., B. Dietzschold, and K. M. Carbone.** Immunopathogenesis of Borna disease. Curr. Top. Microbiol. Immunol., in press.
46. **Stitz, L., O. Planz, T. Bilzer, K. Frei, and A. Fontana.** 1991. Transforming growth factor-α modulates T cell-mediated encephalitis caused by Borna disease virus. Pathogenic importance of $CD8^+$ cells and suppression of antibody formation. J. Immunol. 147:3581–3586.
47. **Stitz, L., M. Sobbe, and T. Bilzer.** 1992. Preventive effects of early anti-CD4 or anti-CD8 treatment on Borna disease in rats. J. Virol. 66:3316–3323.
48. **Stitz, L., D. Soeder, U. Deschl, K. Frese, and R. Rott.** 1989. Inhibition of immune-mediated meningoencephalitis in persistently Borna disease virus infected rats by cyclosporine A. J. Immunol. 143:4250–4256.
49. **Stoler, M., T. Eskin, S. Benn, R. Angerer, and L. Angerer.** 1986. Human T-cell lymphotropic virus type III infection of the central nervous system. JAMA 256:2360–2364.
50. **Street, N. E., and T. R. Mosmann.** 1991. Functional diversity of T lymphocytes due to secretion of different cytokine patterns. FASEB J. 5:171–177.
51. **Stuhler, G., and P. Walden.** 1993. Collaboration of helper and cytotoxic T lymphocytes. Eur. J. Immunol. 23:2279–2286.
52. **Thiedemann, N., P. Presek, R. Rott, and L. Stitz.** 1992. Antigenic relationship and further characterization of two major Borna disease virus-specific proteins. J. Gen. Virol. 73:1057–1064.
53. **Thierer, J., H. Richle, O. Grebenstein, T. Binz, S. Herzog, N. Thiedemann, L. Stitz, R. Rott, F. Lottspeich, and H. Niemann.** 1992. The 24K protein of Borna disease virus. J. Gen. Virol. 73:413–416.
54. **Torsteinsdottir, S., G. Georgsson, E. Gisladottir, B. Rafnar, P. A. P. Isson, and G. Petursson.** 1992. Pathogenesis of central nervous system lesions in visna: cell-mediated immunity and lymphocyte subsets in blood, brain and cerebrospinal fluid. J. Neuroimmunol. 41:149–158.
55. **Wang, C. H., M. Korenaga, F. R. Sacuto, A. Ahmad, and R. G. Bell.** 1990. Intramucosal migration to the epithelium of protective, dividing anti-Trichinella spiralis CD4+ OX-22 cells requires MHC class II compatibility. J. Immunol. 145:1021–1028.
56. **Watkins, B., H. Dorn, W. Kelly, R. Armstrong, B. Potts, F. Michaels, C. Kufta, and M. Dubois-Dalco.** 1990. Specific tropism of HIV-1 for microglial cells in primary human brain cultures. Science 249:549–553.
57. **Wekerle, H., C. Linington, H. Lassmann, and R. Meyermann.** 1986. Cellular immune reactivity within the CNS. Trends Neurosci. 9:271–277.
58. **Wiley, C. A., R. D. Schrier, J. A. Nelson, P. W. Lampert, and M. B. A. Oldstone.** 1986. Cellular localization of human immunodeficiency virus infection within the brains of acquired immunodeficiency syndrome patients. Proc. Natl. Acad. Sci. USA 83:7089–7093.
59. **Wong, G. H. W., P. F. Bartlett, I. Clark-Lewis, F. Battye, and J. W. Schrader.** 1984. Inducible expression of H-2 and Ia antigens on brain cells. Nature (London) 310:688–691.
60. **Zinkernagel, R. M., G. N. Callahan, A. Althage, S. Cooper, J. W. Streilein, and J. J. Klein.** 1978. The lymphoreticular system in triggering virus-plus-self-specific cytotoxic T cells: evidence for T help. J. Exp. Med. 147:897.
61. **Zinkernagel, R. M., M. Eppler, H. P. Pircher, D. Kägi, T. Leist, K. Bürki, B. Odermatt, and H. Hengartner.** 1989. Immune-protection versus immunopathology by antiviral T-cell responses. Prog. Immunol. VII:906–913.